The odd relation between foveal and parafoveal vision.

Shawn Barr

Submitted to the faculty of the University Graduate School

in partial fulfillment of the requirements

for the degree

Doctor of Philosophy

in the Department of Psychological and Brain Sciences

September 2017

Accepted by the Graduate Faculty, Indiana University, in partial fulfillment of the requirements for the degree of Doctor of Philosophy

Doctoral Committee

_____
Jason M. Gold, PhD

_____
Thomas Busey, PhD

_____
T. Rowan Candy, PhD

_____
Chunfeng Huang, PhD

April 27th, 2017

Shawn Barr

THE ODD RELATION BETWEEN FOVEAL AND PARAFOVEAL VISION.

The experiments presented in this thesis explore how our perception of the spatial structure of a pattern changes as the pattern shifts from our central into our parafoveal field of view. These experiments follow up on an important finding that an observer's ability to discriminate between a particular set of patterns could be substantially reduced by changing the local spatial configuration of the pattern from even to odd symmetric (i.e., by changing the *relative spatial phase* information) when the pattern was presented in the periphery (Bennett and Banks, 1987). Yet, despite a number of follow-up experiments (Bennett and Banks, 1991), how these changes in phase information were limiting the observer's performance remained unclear. In terms of the signal-to-noise ratio associated with the observer, limitations were either due to greater uncertainty about the signal (i.e., noise) or to a decline in the observer's ability to make use of the signal information. Since their experiments, several new techniques have been developed to disambiguate these two types of limitations. The experiments in this thesis will employ three of these techniques. One technique was used to measure the amount of internal noise associated with the observer. A second technique was used to determine if this noise level was affected by the contrast level of the stimulus and a third provided an estimate of how efficiently the observer sampled information from the stimulus. Together these techniques showed that, due to a reduction in spatial sensitivity in the parafovea, observers were able to make use of only a limited portion of the signal after changing the spatial configuration of the patterns from even to odd symmetric.

Contents

List of Figures

1 | Introduction

Altogether, these experiments examine how the perception of a pattern changes as it appears farther from the center of the visual field. Studies of visual perception are typically set in the center-most region where visual acuity is the highest. As patterns are shifted beyond this foveal region, visual acuity decreases and patterns become more difficult to distinguish. According to Swanson and Fish (1995), visual regions outside of the fovea such as the parafovea (i.e, 5-8 degrees of visual angle), perifovea (between 8 and 18 degrees of visual angle), and periphery (i.e., beyond 18 degrees) extend our visual field beyond the narrow scope of the central visual field and provide cues as to where to direct attention. However, as the visual scope widens, our ability to locate and identify precise visual characteristics diminishes. A number of studies have been carried out to relate perceptual ability across the visual field. Results from these studies have typically been interpreted in two ways. According to one view, the performance of an observer detecting a signal in the fovea can be matched by scaling the stimulus presented in the periphery by a cortical magnification factor (Rovamo and Virsu, 1979; Koenderink and Doorn, 1978). Others have suggested that low frequency information is preserved as the stimulus is shifted to the periphery, along with some aliased information that falls within a spectral region just above the high frequency cutoff (Thibos et al., 1996). Based on these characterizations, we might

expect that patterns comprised of the same amplitude spectra would be equally discriminable in the periphery. However, Bennett and Banks (1987) found a considerable disparity in the discriminability of two patterns that differed only in their relative phase information. This result suggests that both the amplitude and phase spectra influence the relation between central and peripheral pattern discrimination at higher eccentricities.

Patterns with repetitive elements, such as the ones used in these experiments, can be described by their luminance values across space or based on their phase and amplitude spectrum. The amplitude and phase represent a mapping of the original pattern onto a set of periodic sine and cosine waves, which is accomplished by taking a Fourier transform of the pattern. The amount and arrangement of these trigonometric basis functions necessary to represent the original pattern are defined by the amplitude and phase spectra. For patterns that are highly periodic, the Fourier or spectral domain offers a simplier representation of the pattern. For example, the patterns used in this thesis can be represented by either two cosines or a cosine and a sine. These waves are combined in integer multiples or harmonics of the fundamental frequency. The amplitude and phase indicate the height of each wave and the relative arrangement of the waves necessary to reconstruct the original pattern. This process of breaking apart a signal into its component frequencies has been compared to the way a prism splits light into its constituent colors (Bracewell, 1989).

Since the patterns used in this thesis contained only two components, a fundamental and second harmonic, there was only one phase relation that changed

the relative spatial position between them. Changes in this phase relation can be used to form two types of visual features–bars and edges (Field and Nachmias, 1984). The alignment of the peaks of the two waves resulted in a bar-like feature in the combined pattern due to some squaring at the peak. When the two waves were shifted so that the peak of one wave physically aligned with a zero-crossing of the other, an edge-like pattern was formed. Together, these bar and edge-like features form a basis for more complicated visual patterns. In Figure 1.1 below, the effect of adding together multiple sine waves (the odd harmonics) aligned with one another can be seen. In this alignment, all of the harmonics have the same phase and the result is a square wave. In terms of visual features, this might be considered a pure bar stimulus because the edges make up such a small portion of the stimulus.

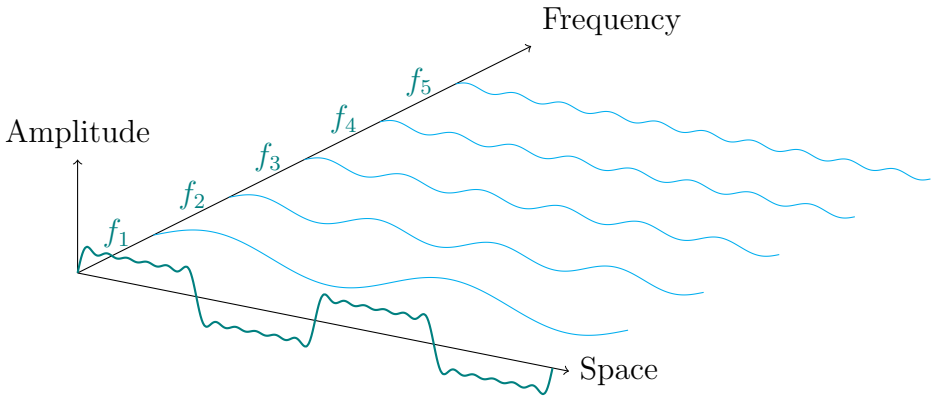

Figure 1.1: Fourier representation of a square wave. The top row shows how increasing the number of Fourier components influences the shape of a square wave. That is, as the series expands to include higher frequencies, the edges sharpen to form a rectangular pattern. In the 3-D plot below, a square wave with 5 components is broken out into its component frequencies. When all of the components are aligned (in phase), they add together to form the bars that make up a square wave.

To provide some intuition about how the phase and amplitude influence the

appearance of a pattern, a square wave and its first five harmonics are depicted above. In this arrangement the peaks and troughs of the waves align to sharpen the features of the waveform. For more complicated patterns, such as a natural image, low frequencies correspond to gradual changes in the pixel intensities across the image and high frequencies to sharper differences across the image. Natural images tend to contain a disproportionate amount of low frequencies. High frequencies within an image correspond to features like an edge or horizon. Compared to the amplitude spectrum, the phase spectrum is more difficult to disambiguate. The starting position of waves of nearby frequency often provides little intuition about the overall appearance of the image. Altering the phase spectrum, however, can completely change the appearance of the image; whereas, the objects within an image may still be recognizable after changing the the distribution of the amplitude spectrum. Oppenheim and Lim (1981) demonstrated this by switching the amplitude and phase spectra from two example images. A similar manipulation was carried out in Figure (1.2) below. Instead of swapping the amplitude spectra, the amplitude and phases were replaced with Gaussian white noise spectra. The importance of the phase information for preserving the overall structure of the image can be seen by comparing the first and last rows of Figure (1.2).

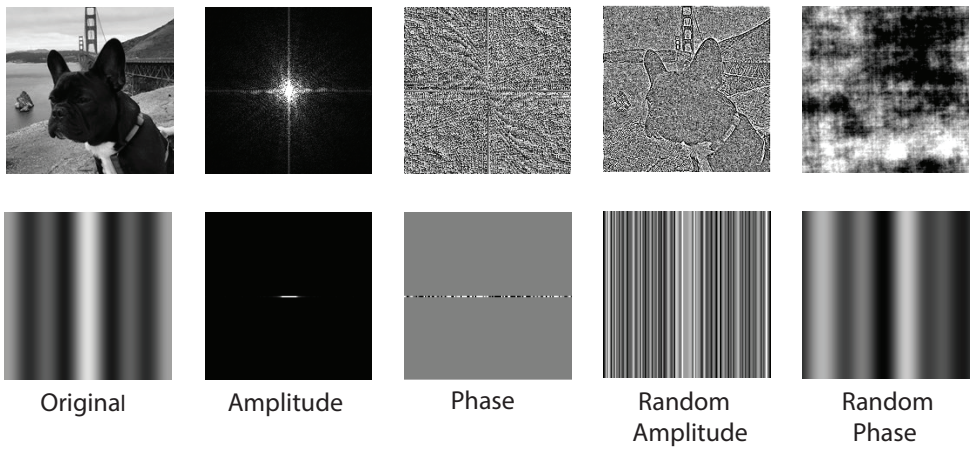

Figure 1.2: Fourier Transform. This figure provides two examples of the amplitude and phase spectra of a natural image (top row) and one of the stimuli used in these tasks (bottom row). The amplitude spectra are centered in the middle of the plot so that the frequency increases away from the center. The concentration of brightness around the center of the amplitude spectrum in the top row indicates a disproportionate amount of low frequency information. Along with some high frequency components that extend out from the center along the horizontal and vertical axes. When the amplitude spectrum is replaced with the amplitude spectrum of a sample of white noise (shown in the random amplitude column), the amplitudes are spread out along the spectrum and the edges outlining the dog become more apparent. When the phase spectrum of the original is replaced with the phase spectrum from a sample of white noise (random phase column), the scene from the top row is no longer recognizable and the presence of low frequencies (gradual changes) becomes (more) apparent. In the bottom row, the example pattern varies in only one dimension. Hence, the Fourier transform can be represented along a single dimension. As expected, the amplitudes are restricted to 2 and 4 cycles/image with some smearing due to the Gaussian envelope. Phase covers the entire spectrum; however, there is no energy associated with higher frequencies. Replacing the amplitude spectrum (column 4) results in a pattern that is very similar to the actual stimulus with noise used in the experiments except that the amplitudes of the first and second harmonic are random. Swapping the phase spectrum (column 5) simply changes the phase relations of the harmonics that contribute energy in the original pattern. Hence, the pattern retains the edge and bar-like features.

1.1 Phase in pattern detection and discrimination

In the late 60s, a model of spatial pattern perception was suggested by Campbell and Robson (1968) that compared the human observer to a Fourier analyzer with multiple frequency–specific channels. This multiple-channel model was based on experimental evidence provided by Campbell and Robson (1968) that the observer's ability to discriminate between a sine and square wave was not based on the overall contrast of the two patterns, but rather by the contrast of the square wave's third harmonic. These authors concluded that observers, like a Fourier analyzer, were able to separate the components of a compound grating pattern.

According to this multiple channel model, a pattern could be detected when any of its harmonic components were visible, and two patterns could be discriminated when at least one harmonic component that differentiated the patterns exceeded their independent detection threshold (Klein, 1992). Further evidence for a multiple independent channel model was provided by Graham and Nachmias (1971) who showed that there was no subthreshold summation between the first and third harmonics. Pantle and Sekuler (1968) found that following adaptation only frequencies that were similar to the adapted pattern frequencies were more difficult to detect, leading to the same conclusion. A similar adaptation effect was also found by Blakemore and Campbell (1969) for size and orientation.

The assumption of channel independence was later called into question as more sophisticated experiments were carried out. For instance, DeValois (1977)

found that detection of the third and fourth harmonics were facilitated by adapting to the fundamental. Tolhurst and Barfield (1978) also found evidence that thresholds were lowered for frequencies beyond 1-2 octaves of the adaptation frequency, and elevated for frequencies within that 1-2 octave band. These interactions suggested that spatial frequency sensitivity depends on the entire amplitude spectrum of the pattern. An alternative account for interactions between channels was that, in addition to spatial frequency information, the relative phase of the components also played a role in pattern discrimination. This possibility was suggested by Stromeyer and Klein (1974) who found that jittering the spatial position of the stimulus reduced the effect of masking. This finding led to other investigations of the aspects of the phase spectrum that influenced the perception of spatial patterns.

Similar to early experiments involving multiple spatial frequency channels, the effect of phase information on the observer's detection and discrimination ability was the first to be investigated. The results of these early experiments confirmed the multiple-channel hypothesis of Campbell and Robson (1968) with regard to detection, but some further refinement was required to account for discrimination. That is, regardless of the phase relations among the patterns components, detection still occurred whenever any component exceeded its detection threshold (Graham and Nachmias, 1971; Huang et al., 2006). For discrimination to occur, the relevant harmonics needed to be sufficiently above detection threshold, as before, provided the following new conditions were met: that a) those harmonics exceeded a minimum phase angle (Nachmias and Weber, 1975), and b) some additional contrast was required for phase angles that were less favorable

for discrimination. For condition a) the value of the minimum phase angle was estimated be between 20° and 30° for a typical observer (Burr, 1980), and as little as 10° for one highly trained observer (Badcock, 1984). Evidence that the observer's discrimination ability depended on the arrangement of the frequency components was provided by (Field and Nachmias, 1984). In their experiments, Field and Nachmias asked observers to discriminate between two patterns that were composed of the same two frequency components: a fundamental (f) and its second harmonic ($2f$). Each of the components had an associated phase angle. The fundamental had phase θ, and the phase of the second harmonic was ϕ. Only θ, which was called the *base phase*, was varied in their experiments. To produce a pair of patterns, the *relative phase* ϕ was fixed at either 0° or 180°. Since a 180° phase shift corresponded to a phase reversal, this experimental technique was referred to a phase reversal discrimination.

The results obtained by varying the base phase angle θ from 0° to 180° followed an interesting pattern. Observers tended to perform best when the base phase was either 0° or 90° and worst when the base phase was 45° or 135°. Field and Nachmias interpreted this periodicity as evidence for a two-channel model in which one channel responded best to the peaks and troughs in the waveform and the other channel was most sensitive to zero crossings in the waveform. When these waves were translated into grating patterns, peaks and troughs resulted in bright and dark bars; left and right edges were formed by the zero crossings in the waveform. To account for their experimental results, Field and Nachmias assumed that only the more sensitive channel was used to perform the discrimination. A diagram of the edge and bar detector channels proposed by Field

and Nachmias is shown is below in Figure (1.3). The portions of the waveform that maximize the responses of each set of filters are highlighted as positive filter responses in Figure (1.3).

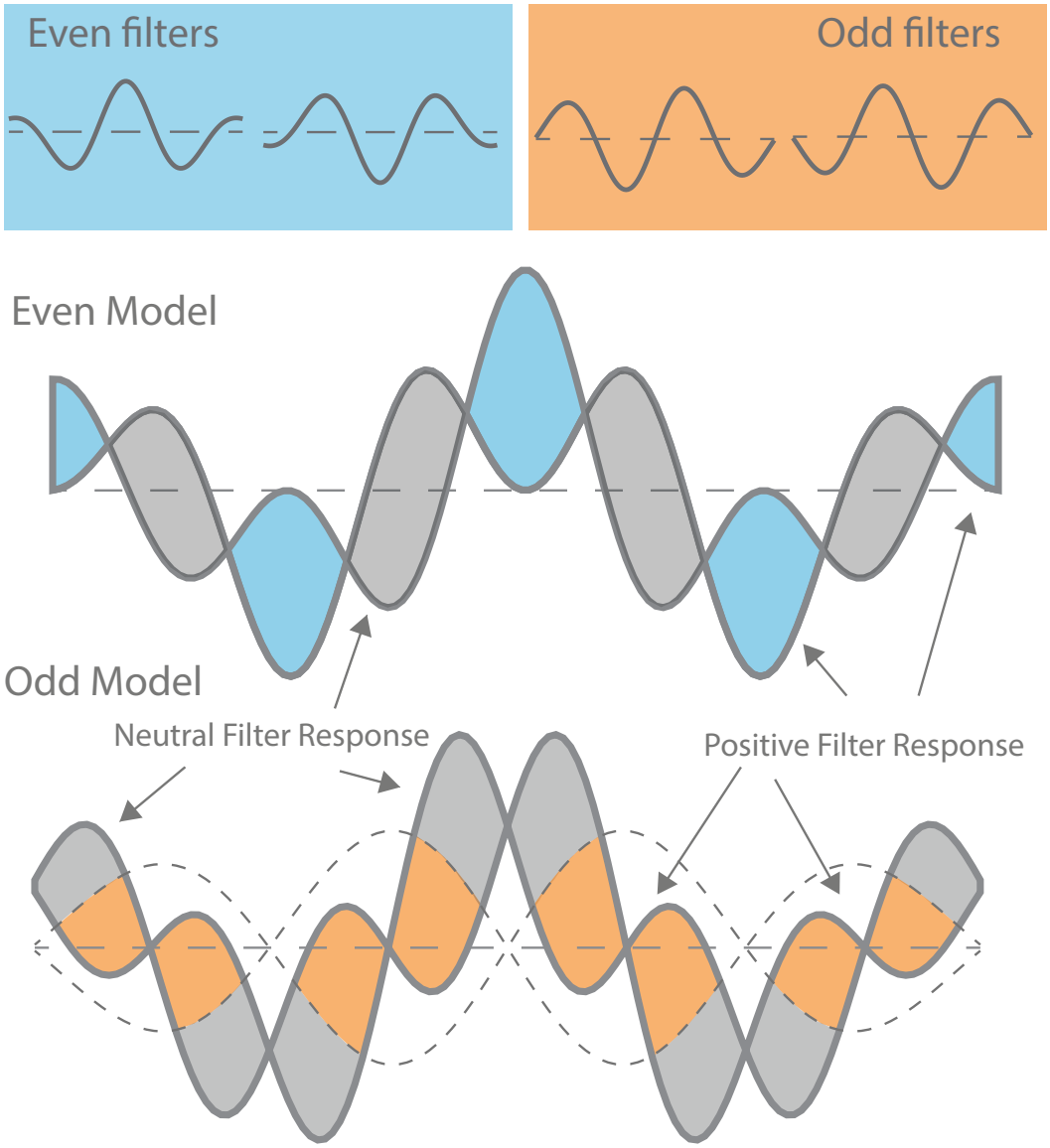

Figure 1.3: Two-channel model. According to the two-channel model proposed by Field and Nachmias (1984) there are two sets of filters tuned to respond maximally to bars and edges. The bar or even filters are sensitive to regions of the pattern that remain above or below background contrast. The dark gray lines represent the contrast profiles of the stimuli used in these tasks. The blue highlighted regions correspond to the even features or bars that the filters detect in the cosine condition. In this condition, the most discriminative regions of the patterns correspond to the peaks and troughs of the contrast profiles. Since the luminance profiles in the cosine condition are mirror symmetric, the phase-reversal discrimination task could not be performed using the response of the odd filters. In the sine condition, the two alternatives cannot be discriminated using the contrasts at the peaks and troughs of the waveform. Instead, odd filters are sensitive to changes in the contrast of the pattern. A sharp change in contrast indicates the presence of an edge. Odd filters respond to differences in the slopes of the contrast profiles. The responses of the odd filter are highlighted in orange.

Consistent with their experimental findings, the set of cosine filters that responded to bar-like features was most sensitive to a stimulus pair with a base phase of 0°. This pair is the Even Model example depicted in Figure 1.5. The Odd Model example in the panel below shows a stimulus pair whose base phase is 90°. As the base phase angle varied from 0-45°, some of the discriminative information shifted from the cosine (even) to the sine (odd) channel. Since Field and Nachmias varied the contrast of the second harmonic to determine the observer's discrimination threshold, the contrast associated with the sine and cosine portions of the observer's threshold can be determined by the following angle addition identity:

$$\cos\theta + \phi = \cos\theta\cos\phi - \sin\theta\sin\phi. \tag{1.1}$$

According to this identity, the observers threshold (a) decomposes into orthogonal sine and cosine components: $a\cos\theta$ and $-a\sin\theta$. This two-channel model assumed that, for any θ, a fixed amount of contrast was necessary to satisfy the discrimination threshold of each channel. As θ increased from 0 to 45, the predicted amount of additional contrast necessary to reach the threshold formed a box pattern, shown in Figure (1.4), when the threshold was plotted in polar coordinates. That is, when the sine and cosine portions of the observer's contrast threshold were plotted on the x- and y-axis, the two-channel model predicted that the observer's threshold will increase in constant proportion to the amount of additional contrast necessary reach the threshold for that channel.

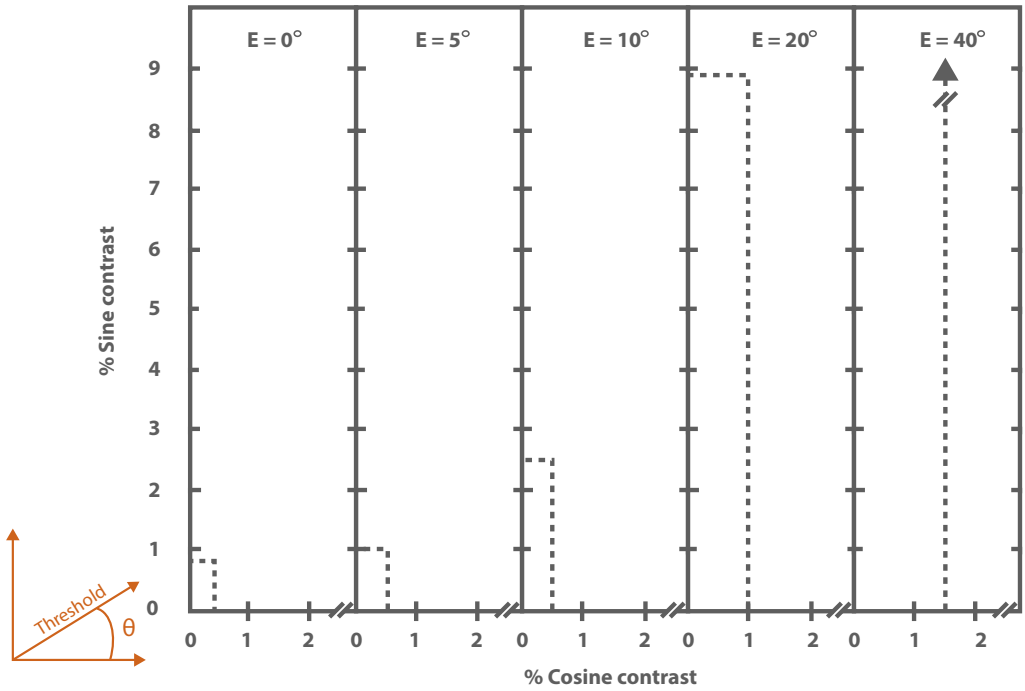

Figure 1.4: Reproduced results from Bennett and Banks (1987). Following the orange diagram on the right, thresholds were plotted in polar coordinates according the magnitude and phase angle (θ) between the first and second harmonics. Moving from left to right eccentricity increased from $0-40°$. Data from their experiments tended to fall along the dotted lines, which represents the predictions of a model that uses the proportion of information available to the more sensitive channel. Straight lines indicate that this proportion remained constant regardless of the phase angle. The scale of the plots helps to visually reduce the effect of noise at smaller eccentricities.

Around the time of that Field and Nachmias conducted their phase-reversal discrimination experiments, hypotheses were being tested to relate the central and peripheral visual fields. Similar techniques were being applied to test how detection and discrimination were affected by shifting the presentation of a pattern beyond the observer's central visual field.

1.2 Non-central vision

Before going into the experimental findings on how psychophysical performance changes in the periphery, consider a brief background on the regions of the visual field. Throughout this thesis, and in parts of the literature, the terms fovea and periphery are used to differentiate between qualitatively different visual regions. Loosely speaking, there is a marked loss in resolution and spatial sensitivity when transitioning from the central to peripheral visual field. As this transition occurs, the absorption of light shifts from a high density of cones in the fovea to rods, which grow increasingly sparse as eccentricity increases. This decrease in photoreceptor density results in a reduction in the stimulus frequencies that can accurately be represented by the photoreceptor mosaic, down from 50-60 cycles/degree of visual angle in the fovea to about 3-4 cycles/degree in the periphery (Thibos and Bradley, 1991). In many of the experiments described thus far, and in all of the experiments presented as part of this thesis, stimulus presentations never reach as far as the periphery. According to Swanson and Fish (1995), the periphery doesnt begin until 18 degrees of visual angle. Two intermediate regions, the parafovea, which extends from 5-8 degrees of visual angle, and the perifovea, which falls between the parafovea and periphery, separate the fovea and periphery. A full diagram of the regions of the visual field is provided in Figure (1.5) below. In terms of performance on psychophysical tasks, these intermediate regions tend to have more in common with the periphery than the fovea. For example, Levi and Klein (2002) found that observers' thresholds doubled at an eccentricity of only 2 degrees. Hence, the use of periphery in place of parafovea, the technically accurate region of the visual field, is simply meant to

refer to the qualities of the visual field shared by regions visual regions beyond the fovea.

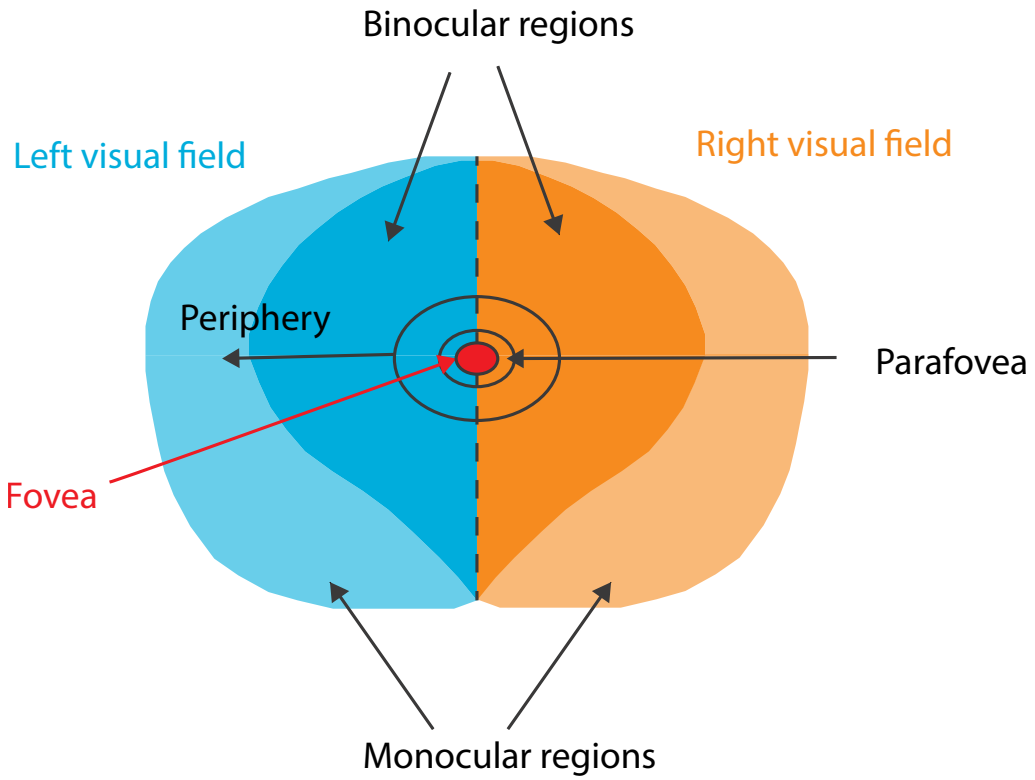

Figure 1.5: Visual field. Modeled after a textbook figure that appears in Purves et al. (2001), this figure shows the visual field that results from the overlap between the visual fields of the left and right eyes. An estimate of the boundaries that separate the Fovea, Parafovea, Perifovea, and Periphery are indicated. The shape of the regions in figure below matches the textbook description provided by Purves et al. (2001). The asymmetry at the bottom of the in the binocular regions reflects some obstruction from the nose. Due to physiological constraints of the eye, the width of the visual field is also greater than the height. Another technical term that is used throughout this thesis is eccentricity. Eccentricity is the degree of horizontal shift away from the center of the visual field, i.e. into the horizontal nasal field.

In general, psychophysical performance tends to be worse under peripheral viewing conditions. Detection and discrimination thresholds tend to increase considerably when the stimulus presentation is shifted beyond the center-most

visual region. For example, Harvey et al. (1985) found that contrast thresholds for detecting a checkerboard pattern were roughly double at just 2° eccentricity. These authors also found that, at the same 2° eccentricity, the minimum phase angle necessary to discriminate a pair of patterns increased by about 3.8 times– from 35° to 140° on average. Discriminations of two-component grating patterns ($f + 3f$) also followed a similar trend when presented 2° in the horizontal nasal field (Rentschler and Treutwein, 1985). These authors found that peripheral deficiencies with patterns differing in the maximum and minimum contrast could be accounted for by a scaling the signal by a cortical magnification factor across eccentricities; however, differences with mirror (odd) symmetric patterns were not consistent with a simple scaling account.

Bennett and Banks (1987) investigated phase reversal discriminability of two-component grating patterns ($f + 2f, f - 2f$) in the fovea and at 5°, 10°, 20°, and 40° eccentricity using a procedure similar to Field and Nachmias (1984). The two-channel model used by Field and Nachmias to account for their results was also consistent with the findings of Bennett and Banks, provided that the feature detectors were able to locate the places in the waveform where the features occurred. As pattern presentation was shifted further into the periphery, the two points necessary to compute the model prediction (i.e., the contrasts necessary for pure edge and pure bar discriminations) grew disproportionately to one another. When stimulus presentations were shifted by 10°, the contrast necessary to discriminate an odd-symmetric pair was about 2.5 times greater than for an even-symmetric pair; however by 20°, odd pairs required nearly 9 times more contrast than even pairs.

Bennett and Banks (1991) discuss some possibilities to account for this disparity between peripheral discrimination of odd and even symmetric patterns. According to one possibility, stimuli presented peripherally and centrally differ by a cortical magnification factor (Hubel and Wiesel, 1974; Rovamo and Virsu, 1979) and sine and cosine signals were scaled by different factors. The increase in the odd-even ratio, however, was greater than this linear prediction, suggesting that the change in performance across the two channels as stimulus presentations were shifted into the periphery could not be related by a common factor. Another possibility to account for a non-linear even-odd ratio was a compression of the waveform introduced during the early stages of visual processing. Since an odd-symmetric waveform is mirror symmetric, this compression would not affect the relative contrast of the sine pair and would lead to a monotonic change in the odd-even ratio as the fundamental contrast increased. However, adjusting the fundamental contrast did not appear to systematically change the odd-even ratio. Despite these possibilities, Bennett and Banks (1991) were not able to provide an adequate account of the increasing change in the odd-even ratio.

1.3 Signal and noise in phase reversal discrimination

The goal of the experiments presented in this thesis was to investigate whether the dramatic deficiency with sine phase information in peripheral vision reported by Bennett and Banks (1991) was due to an increase in the amount of internal noise associated with the observer or a decrease in the observers ability to extract information from the stimulus.

Since Bennett & Banks' original set of experiments, several new techniques have been developed to determine the additional limitations faced by observers in the sine condition. These techniques, which are based in signal detection theory, involve introducing noise to the signal to determine the source of the observer's inefficiency. According to signal detection theory (Green and Swets, 1966) observers are assumed to respond probabilistically to a given stimulus. Consequently, in an experiment where the observer is asked to detect a signal in noise, the observer's responses can be represented by two separate distributions: one for signal plus noise and one for noise alone. The separation between these two distributions (in units of standard deviation) is defined as the observer's sensitivity or d'. Changes in sensitivity can arise from differences in the signal or noise portion of this ratio (Pelli and Farell, 1999). Measuring human performance in terms of the signal energy plus internal noise has several advantages over other measures of performance such as percent correct. For one, it leads to an unbiased estimate of the observer's performance. That is, measuring performance in terms of the signal to noise ratio required by the an optimal or 'ideal' observer to match the performance of the human observer does not depend on whether the observer is more likely to choose one response over the other (Tanner Jr and Birdsall, 1958; Green and Swets, 1966). This measure, d', is depicted in the figure below. In a typical signal detection task, such as the one below, the observer is asked to detect the presence or absence of a signal added to noise. The observer's response to noise alone is assumed to produce a distribution of responses centered on μ_n. Adding a signal to the noise produces a shifted distribution of responses centered on μ_s. For simplicity, the distributions are assumed to have the same standard

deviation (σ). d' is a measure of how far the signal shifts the distribution in units of σ. Whether the observer answers "yes" or "no" to having detected the signal depends on whether the observer's response exceeded the threshold, shown in green.

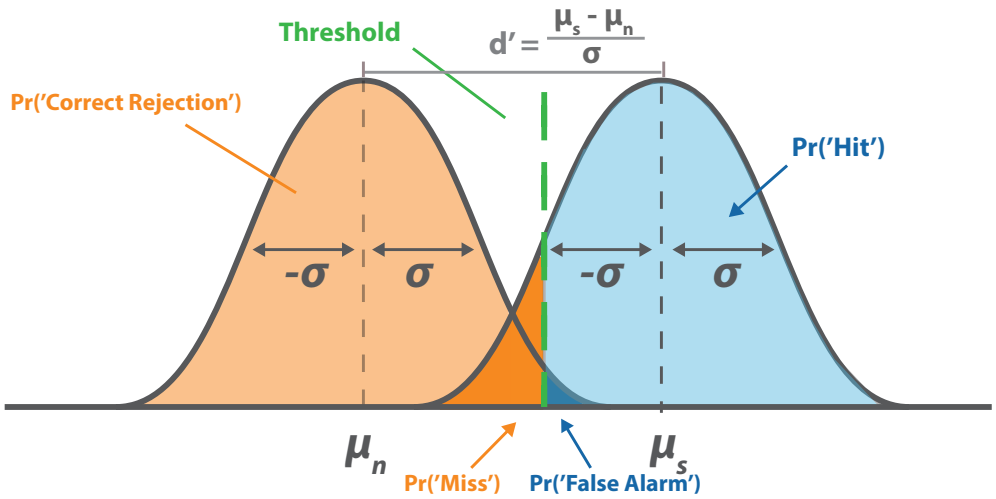

Figure 1.6: Signal detection task. The four possible outcomes that result from a yes-no detection task are depicted. A Hit occurs when the signal is correctly detected; likewise, a correct response to the absence of the signal is a Correct Rejection. When the signal is present but not detected, a Miss (or type II error) occurs, and when the observer responds signal when only noise was present a False Alarm (or type I error) occurs. d' can also be calculated as the difference between the light and dark blue regions, i.e., $d' = Z(Hit) - Z(FA)$.

Another advantage of using d' is that, taking the ratio of human to ideal performance provides a measure of how efficiently human observers made use of the signal information. This efficiency measure provides a control for the intrinsic task difficulty, and can therefore be used to compare the performance of human observers across tasks that differ in the amount of information contained by the signal. Without this control, the intrinsic difficulty of the task remains a potential

confound if the amount of signal information is not balanced across experimental conditions.

In order to specify how each component of this ratio contributes to differences in d' (e.g., differences between d' for sine vs. cosine phase shifts), some assumptions about the observer are necessary. According to (Pelli, 1981; Pelli and Blakemore, 1990), observers are limited by an irreducible source of internal variability that is contrast-invariant and adds to the observer's internal representation of the stimulus. A decision is reached by performing a contrast-invariant calculation on the observer's representation of the signal plus internal noise. This calculation determines how efficiently the observer samples information from the stimulus. These assumptions are used to construct a black-box model of the observer.

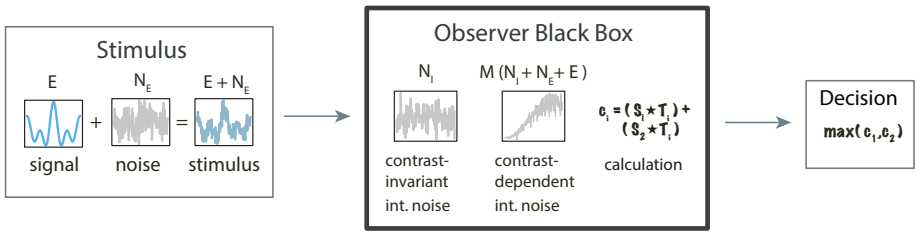

Figure 1.7: Black box model. According to the black box model, the signal is transformed into a response by a contrast-invariant calculation. Noise is introduced prior to the calculation. A more detailed description of the calculation is provided in the methods section.

To determine how the contrast-invariant portions of this ratio change, the signal is embedded in a sample of external noise. An estimate of the observer's

internal noise can be made by varying the noise spectral density (NSD) of this external noise sample to reveal at point at which the internal and external noise levels are equivalent (Pelli and Blakemore, 1990). Since the two noise sources are assumed to be independent, changes in the observer's ability to perform the task will be gradual in regions where there is a large disparity between internal and external noise and more pronounced as the two levels reach parity. That is, at low levels of external noise contrast the observer's internal noise limits performance, and as the noise level increases, the contribution of each noise source to the total amount of noise evens out until eventually the external noise outweighs the internal noise. A plot of the observer's contrast energy threshold against noise spectral density (a *noise-masking function*) reveals a point at which the internal and external noise levels are assumed to be equivalent. This equivalent noise is also the level of external noise necessary to double the observer's threshold. The shape of the noise masking function is also diagnostic of whether changes in performance are due to the contrast-invariant signal or noise portion of the observer's sensitivity. A shift in the equivalence point indicates a change in internal noise. Whereas for a change in the portion of total stimulus energy available to perform the task or sampling efficiency, the equivalence point remains fixed and the intercept of the function is shifted.

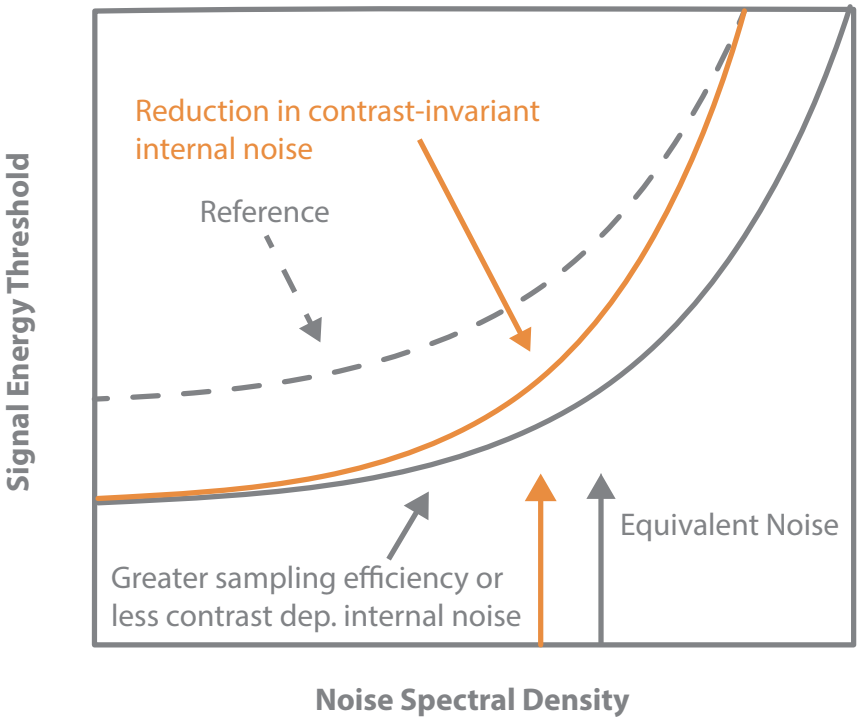

Figure 1.8: Hypothetical noise masking function. Plotting the noise spectral density against the threshold energy in log-log coordinates reveals the observer's equivalent noise, i.e., the point that maximizes the change in slope of the function. Relative to a reference observer with some level of internal noise and imperfect sampling efficiency, depicted by the dashed line, a reduction in the contrast invariant internal noise level results in a leftward shift in the elbow of the function (shown by the orange line); and an improvement in calculation efficiency leads to a downward shift in the noise masking function, indicated by the solid gray line. Gold et al., (2004) observed such an effect as a result of perceptual learning. An upward or downward shift in the noise masking function can also be due to a change in the contrast-dependent noise source.

A second possibility also exists to account for the change in the slope of the noise masking function. Burgess and Colborne (1988) found evidence that the internal noise level grows in proportion to the external noise level. This suggests that internal noise has a fixed contrast-invariant component and a second component that is proportional to the external noise level. An estimate of the

contrast-dependent component of internal noise can be obtained by using a response consistency procedure (Burgess and Colborne, 1988; Green and Swets, 1966). This technique works by repeating the same sequence of noise through a second pass of trials. The responses of an observer without internal noise would be the same for both presentations of identical noise. However, since human observers are also limited by internal noise, their responses to the same stimulus will be different on some portion of the trials. These response inconsistencies along with the proportion of correct responses can be used to provide an estimate of the observers internal to external noise ratio. At high levels of external noise, the contrast-invariant component of internal noise will be small relative to the contrast-dependent component. Therefore, measurements of response consistency can be used to determine the contribution of contrast dependent noise to the total internal noise limiting human observers. Once an estimate of the internal noise has been provided, any changes in sensitivity that are not due to a combination of contrast-invariant and contrast-dependent internal noise are due to a change in the sampling efficiency. While increased noise suggests that performance is degraded evenly (on average) across all parts of the image, differences in sampling efficiency suggest systematic changes in observer's use of stimulus information and may be associated with a change in strategy. For example, the observer may shift their attention to less informative regions of the stimulus or even introduce new features into uninformative regions of the stimulus (Gold et al., 2004).

Changes in sampling efficiency can be mapped directly onto the stimulus by using a reverse correlation technique to provide an estimate of the observer's

underlying template. Reverse correlation works by averaging the noise fields for each of the possible responses and combining them to form a map of the individual pixel weights (Ahumada, 2002). This estimate of the observer's underlying template can then be used to identify regions of the stimulus that are more highly correlated with a particular response. The spatial distribution of weights can also be thought of as a behavioral estimate of the observer's receptive field used to perform the task. This technique can also be applied in the frequency domain to provide an estimate of the amplitude and phase spectrum associated with an observer's underlying template (See Murray (2011) for a complete review). Levi and Klein (2002) used this technique to compare detection and discrimination of sine wave patterns in the fovea and parafovea. Their results showed that observers tended to over weight high frequency components in the fovea and low frequency components in the periphery. These weightings suggest differences in the receptive field shape between the fovea and periphery.

1.4 Summary of Goals

Overall, this research aims to provide a more complete account of the factors affecting discrimination of a pair of spatially modulated sinusoidal grating patterns and the deficit that arises for odd-symmetric patterns viewed at higher eccentricities. While detection of these types of patterns is typically assumed to be limited only by contrast energy, phase has also been shown to be an important predictor of the discriminability between two equal energy gratings. For some grating pairs, the role of phase becomes more pronounced as gratings are shifted into the periphery where spatial sensitivity is reduced. By using a com-

bination of techniques that rely on the use of external noise, an estimate of the observer's calculation efficiency and internal noise can be provided. These two characteristics of the observer determine the additional limitations faced by the observer due to changes in the spatial configuration of the pattern. In the next chapter a more detailed account of the methods used to carry out these experiments will be provided, followed by a summary and discussion of the results in the third chapter.

2 | Methods

The purpose of this chapter is to provide a general account of the methods used to carry out the experiments presented in this thesis. Details specific to each of the experiments are presented in the next chapter. Overall, these experiments were designed to match, as closely as possible, those presented by (Bennett and Banks, 1987, 1991). The major difference between these experiments and those of Bennett and Banks was that the methods described in this chapter relied on the use of added external noise. This additional limitation placed on the observers in these experiments also meant that performance could not be measured at the same eccentricities used by Bennett and Banks, since performance degraded more quickly in the presence of noise. Another minor difference was the measure of contrast used. Whereas Bennett & Banks used Michelson contrast, the analyses described in this chapter required a different measure of contrast to provide an estimate of the signal energy. Bennett & Banks also varied the contrast of the third harmonic to obtain a threshold estimate, which changed the relative contribution of each harmonic to the overall pattern contrast. To prevent the underlying shape of the signal from changing across contrast levels, the contrasts of both harmonics were varied in equally in these experiments to estimate thresholds. These changes, however, did not prevent any comparisons between performances in the two conditions, which was the critical index of performance

used in these experiments. Aside from these details, the experimental stimuli and the pattern of results were consistent with the original results presented by Bennett and Banks. Moreover, the addition of noise allowed several more recent techniques to be applied, which provide new insights into the factors limiting observers under peripheral viewing conditions.

2.1 Apparatus

Experiments were performed on a 2.3 GHz, dual-core Mac Mini running the Psychophysics Toolbox Version 3.0.8 Brainard et al. (2002) from MATLAB (R2008b). Stimuli were displayed on a 17" Apple Studio Display at a frame rate of 85 Hz, with a resolution of 1024 x 768 pixels. The monitor was calibrated using a Minolta LS-100 photometer. The purpose of calibration was to ensure that luminance produced by the monitor matched the intended luminance as closely as possible. Participants viewed the stimuli displayed on the monitor through natural pupils at a distance 114 cm. At this distance, the display region of the monitor extended 18.55° of visual angle along the horizontal axis and 14° along the vertical axes. A chinrest was used to stabilize the participant's head and to ensure the correct viewing distance. The background luminance of the display was set to 49.7 cd/m^2, and luminances were displayable within the range 5-120 cd/m^2.

2.2 Observers

Due to the extended nature of these experiments, four observers were trained for these experiments. All of the observers had previous experience with psy-

chophysical tasks. Each of the observers gave informed consent and three of the observers were compensated $10/hr for their participation. To preserve anonymity, the four observers were assigned a the following unique ids: s04, s10, s14, and s21. Two of the observers were emmetropes, s04 and s10; s14 wore glasses, and s21 wore contacts while participating.

2.3 Stimuli

Two pairs of two-component grating patterns (4 total) were used as stimuli in the experiments. The stimuli were generated by combining two sinusoidally modulated grating patterns to form a "compound" grating. The modulation of pixel intensities occurred only horizontally across the 128 x 128 pixel (3.875° x 3.875°) stimulus region. All four patterns could be represented by a Fourier series containing a fundamental (f) and second harmonic ($2f$) components. To isolate the effect of phase, the amplitudes of both harmonics and the phases of the fundamental were the same across all four patterns. Consequently, any differences between the patterns in the Fourier domain were restricted to the phase of the second harmonic. (As will be described later, negligible differences between the sine and cosine pair were introduced by the use of a Gaussian envelope.) A fundamental frequency of 2 cycles/image was used to generate all four grating patterns, and the starting position of the fundamental was 90° or cosine phase. To ensure that the fundamental was symmetric across the left and right halves of the stimulus, the origin of the fundamental was set to the center of the stimulus.

To maximize the discriminability of each pair, the phase angles were set to

be 180 degrees apart. A 180-degree difference in the phase angle corresponded to a change in the sign of the waveform or a phase reversal. Accordingly, adding the second harmonic in positive and negative sine or cosine phase formed the two sets of stimulus pairs. The stimuli that resulted from these combinations are shown in the figure below. For convenience, the stimuli are often referred to in shorthand: $f + 2f_{cos}, f - 2f_{cos}$, where f and $2f$ refer to the fundamental and second harmonic with a subscript denoting the phase.

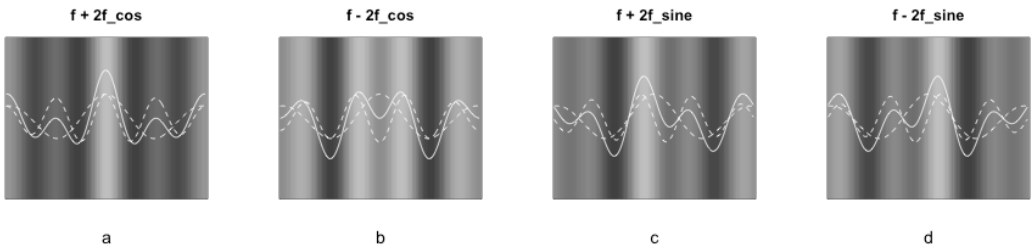

Figure 2.1: Experimental stimuli—cosine pair (a, b) and sine pair (c, d). The fundamental and second harmonic are plotted as dashed lines; their combination is shown as by the solid line. These lines have been overlaid on a high-contrast version of actual compound grating patterns used in the experiments.

In positive cosine phase (figure 2.1a above), the peaks of both harmonics were aligned, resulting in a peaks add combination. A peaks subtract combination was formed in part b above, where the peaks of the f and the troughs, or minima, of $2f$ aligned. The sine pair (parts c, d above) was formed by adding and subtracting a second harmonic that had been shifted 90° into sine phase. When the first and second harmonics were orthogonal, the peak of f was aligned with the point on the second harmonic where the contrast changed sign, i.e., a zero crossing. Reversing the phase of the second harmonic added in sine phase produced a mirror image of the pattern. In the mirror image pair, when a phase reversal occurred, a zero-crossing that went from negative to positive contrast was flipped

to a positive to negative contrast change.

As was mentioned in the previous chapter, the terms odd and even-symmetric pair are used interchangeably with sine and cosine pair. This usage reflects the odd symmetry of the sine and even symmetry of the cosine function. The ratio of the thresholds obtained for the even pair of stimuli to thresholds obtained for the odd pair is defined as the odd-even ratio. Since the signal energy required by the ideal observer is equivalent in the two conditions, the odd-even ratio is a direct comparison of the efficiencies—i.e., the ratio of human to ideal contrast energy threshold—in the two conditions.

In order to ensure that the second harmonic was above detection threshold, the amplitude of the second harmonic was set equal to the amplitude of the first harmonic. While Bennett and Banks (1991) found that varying the contrast of f between about .02 and .9 (in Michelson contrast units) did not change the relative discriminability (odd-even ratio) of the two pairs for well-trained observers, pilot test results suggested that, in the presence of noise, threshold estimation under parafoveal viewing conditions was more problematic with smaller $f : 2f$ ratios. To reduce edge effects, stimuli used by Bennett and Banks (1987) were also multiplied by a Gaussian envelope (the $G(c, \sigma)$ term in the equation below) whose radius at half amplitude equaled one cycle of the wave. For the present task, this corresponded to $\sigma = 54$ pixels or 1.02° of visual angle in the equation below. The envelope was centered on the midpoint of the stimulus (c). The contrast profile of the stimuli can also be expressed by Equation () below. The contributions of the fundamental and second harmonic are represented by the two terms in

the numerator. As mentioned before, the amplitudes of the first and second harmonic share a single coefficient a, which was set equal to .2. The term for the stimulus size s in the denominator normalizes the contrast profile to fit within the boundaries of the stimulus,

$$c(x) = \frac{a\cos(2\pi x) + a\cos(4\pi x + \theta)}{s} \cdot G(c, \sigma) \tag{2.1}$$

By generating stimulus pairs that were composed of the same Fourier components, the total signal energy available to perform the task was effectively the same for the sine and cosine pairs. The figure below highlights the differences in the informative regions between the pairs. Based on the stimulus design, integrating the shaded regions below is equivalent to doubling the amplitude of the second harmonic. That is, when one phase reversed alternative is subtracted from the other, the fundamentals cancel out and the second harmonics (one positive and one negative) add together. In shorthand: $(f + 2fcos) - (f - 2fcos) = 2(2fcos)$.

2.4 Experimental Design & Task

The experiments were designed to match the details of the phase reversal discrimination tasks performed by Bennett and Banks. Consistent with their protocol, a same-different, two-interval forced choice task (2IFC) task was used. Accordingly, participants were instructed to indicate whether the two signals presented sequentially were the same or different. Since a different sample of noise was added to each of the stimuli, the two stimuli always appeared to be different. Hence, observers were instructed to use, as best as possible, only the underlying signal as the basis for their decision.

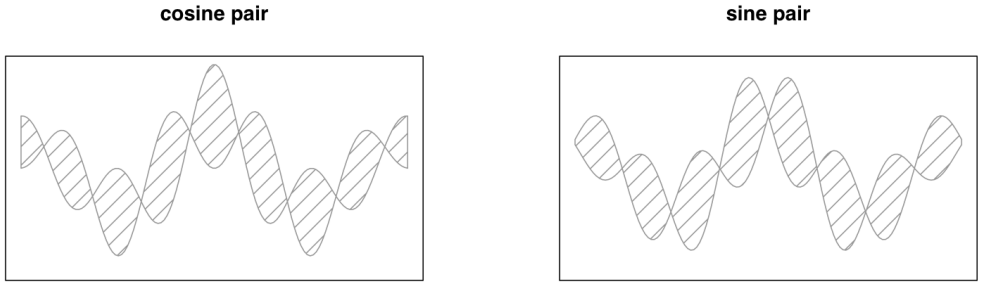

Figure 2.2: Differences between the stimulus pairs. The shaded areas indicate where the contrast profiles of the stimulus pairs differ. The influence of the fundamental (2 cycles/image) is apparent in both the left and right panels. The differences are largest in the center of the image due to the effect of the Gaussian envelope. For the cosine pair on the left, the peak at the center of the "peaks add" profile contains contrast values that exceed the maximum value of the "peaks subtract" profile; the opposite is also true of the minimum value. Unlike the pair on the left, the extreme values do not provide any indication of the phase of the second harmonic. However, dividing the image in half vertically does provide some local clues, which will be discussed later.

Experiments were typically divided into blocks of 250 trials. A trained observer was able to complete a block of trials in about 10 minutes. To familiarize participants with the stimuli and procedure, 16 practice trials preceded each experimental block. At the beginning of the practice segment, the stimulus duration was extended and the noise level lowered to ensure that the details of the stimuli were visible. As the practice segment progressed, the noise was increased and the stimulus duration shortened until they reached the levels used during the experimental block. Participants that were familiar with the stimuli and task could elect to skip the practice block.

To draw attention to the center of the screen, each experimental trial began

with a fixation cross flickering at 20 Hz. The cross remained on the screen for between 150-650 ms (uniformly distributed in increments of 11.8 ms). The first stimulus interval followed the fixation cross and lasted 250 ms. An inter–stimulus interval (ISI) of 250 ms separated the first and second stimulus presentations. The second stimulus presentation also lasted 250 ms. Responses were collected after the second stimulus interval. Participants were reminded of the response options at the bottom of the screen. The choices were 1 = Same and 2 = Different. Auditory feedback was provided after each response: a high-pitched beep indicated a correct response, and a low pitch sounded following an incorrect response. The next trial commenced once a response had been collected, and there was no time limit to respond. Note that the time intervals given here are approximate since the monitor refreshed every 11.8 ms.

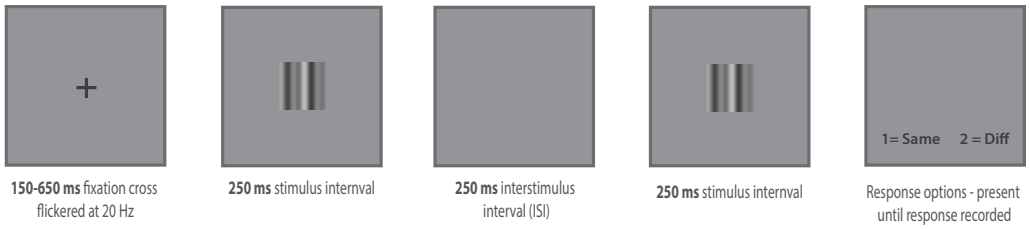

Figure 2.3: Schematic of an experimental trial for stimuli presented in the fovea. The sequence above progressed from left to right. The description below each frame indicates the duration that the frame was displayed.

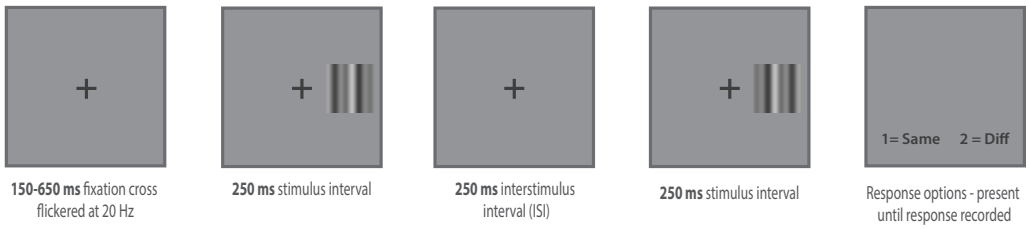

Figure 2.4: Schematic of an experimental trial for stimuli presented in the parafovea. The sequence followed the same progression as above (left to right). The duration of each stage of the sequence is indicated below the frame. In the actual experiments noise was added to the stimuli. Unlike the sequence above, the fixation cross persists throughout the experimental trial in the sequence below. All other details of the trial, other than the presence of noise and the placement of the stimulus, were unchanged.

The procedure was modified slightly when the stimulus appeared in the parafovea. Since no physical constraints were placed on the observer to ensure that they did not shift their eyes to the stimulus location, the fixation cross remained on, in the center of the screen, for the duration of the trial.

2.5 Contrast

The contrast at each pixel in these experiments was defined according to its Weber contrast using Equation (2.2) below. Weber contrast (c_w) is a measure of the distance between each pixel luminance (I) and the background luminance (I_b) in units of the background luminance. The sign of the Weber contrast indicates whether a pixel's luminance is above or below the background luminance (49.7 cd/m^2). Since the luminance cannot be negative, the minimum contrast value is -1, and the maximum value is constrained by the monitor,

$$c_w = \frac{I - I_b}{I_b}. \tag{2.2}$$

To determine the contrast of the entire the stimulus, the root-mean-square (RMS) contrast was computed using the Weber contrast at each pixel. By setting the background contrast to zero, as was specified above by the Weber contrast, the RMS contrast is equivalent to the standard deviation of contrasts across the stimulus according to Equation (2.3) below,

$$c_{RMS} = \sqrt{\frac{1}{N}\sum_{i=0}^{N-1} c_i^2} \tag{2.3}$$

Unlike Michelson contrast, which takes into account only the extreme contrast values, RMS provides an overall measure of contrast that incorporates each pixel. Therefore, regions of the stimulus that do not exceed the maximum or minimum contrast, like the smaller peaks and troughs of a compound grating, are not reflected in the Michelson contrast but do factor in to the RMS contrast. Another reason for favoring RMS, over other measures of contrast, is that the amount of stimulus energy or information provided by the stimulus, which is essential for the methods employed in these experiments, can be computed directly from the RMS contrast. Bennett and Banks, however, did not use noise in their experiments and opted to measure contrast according to the Michelson definition. A comparison of thresholds measured using Michelson and RMS contrast is difficult because there is no direct mapping of values between the two types of contrast (Peli, 1990). These concerns can be avoided, however, by comparing the odd-even ratio across experiments, as taking the ratio of two thresholds factors out the contrast units associated with the threshold.

2.6 Noise

The methods used in these experiments all rely on the use of noise externally added to the stimulus. The type of noise relied upon was Gaussian, white noise. Gaussian, white noise is preferred because it is uncorrelated in both the spatial and frequency domains. Samples of noise were generated using a pseudo-random number generator in MATLAB. Due to the physical limitations of the monitor, some constraints were placed on the noise. To avoid saturation, any noise sample that exceeded 2 standard deviations was resampled until it fell within 2 standard deviations of the mean contrast. Given these boundary conditions, noise added near the peaks and troughs of the waveform was more likely to shift the values closer to the mean contrast than away from it. A different sample of noise was added to each of the two stimulus intervals. Noise was converted into its corresponding noise energy per unit bandwidth by Equation (2.4) below. This was achieved by multiplying the variance of the noise sample (σ^2) by the area of each pixel (a) to produce the total energy or noise spectral density (N) associated with the noise sample,

$$N = \sigma^2 a \tag{2.4}$$

Since the task in these experiments involved two samples of independent noise, the variance in the equation above was the sum the variances from each sample $\sigma^2 = \sigma_1^2 + \sigma_2^2$.

2.7 Threshold estimation

In psychophysical studies, the performance of the observer is typically represented by a unique point along the observer's psychometric function. This point marks a threshold, below which, the observer can no longer reliably perform the task. The slope of the psychometric function is indicative of how much uncertainty is associated with the threshold estimate. When the slope of the psychometric function is steep, there is little uncertainty about the contrast associated with the observers threshold since a sharp change in performance occurs; however, when the slope is shallow, the threshold is more uncertain and may fall within a wide range of contrast values. Psychometric functions are typically fit using either the cumulative Gaussian or Weibull distribution. Both distributions contain a location and scale parameter. In these experiments a Weibull distribution was used to fit the psychometric function. One reason for preferring a Weibull over a Gaussian distribution is that the location and scale parameter, α and β, correspond to estimates of the threshold and slope of the psychometric function (Knoblauch and Maloney, 2012). The Weibull function below gives the probability of a correct response as a function of the contrast energy E,

$$p(E) = 1 - \exp\left(-\left(\frac{E}{\alpha}^{\beta}\right)\right) \tag{2.5}$$

To measure the psychometric function, a staircase procedure was used to bias the stimulus contrast displayed throughout the course of the experiment into a range around 71% correct (see Staircase Procedure below). The actual threshold was estimated from Equation (2.5) above to correspond to a value of 71% correct.

2.8 Staircase Procedure

As mentioned above, an adaptive staircase procedure was used to hone in on the region of stimulus contrast where performance improved the most. To accomplish this, the contrast on each trial of the experiment was adjusted according to a 2-down, 1-up rule (Levitt, 1971). That is, the contrast was lowered following 2 successive correct responses and raised after a single incorrect response. The steps of the staircase were logarithmically spaced to mimic the contrast intervals necessary for the observer to detect a difference. For consistency, the same staircase levels were used in all conditions, and all experiments began at the same place in the staircase. To accommodate large differences in threshold across conditions, the staircase covered a wide range of displayable contrasts. Staircase procedures have some key advantages over other methods of threshold estimation, such as the method of constant stimuli where the number of trials at each contrast level is determined in advance. One benefit from using a staircase procedure is that a threshold can be estimated in fewer trials by biasing the selection contrast values away from levels that are too easy or too difficult for the observer. A second advantage is it takes the guesswork out of having to select contrast values that will be suitable for multiple observers, assuming such values even exist. Hence, the staircase method is considered to be more flexible than other methods, particularly when there are large differences in sensitivity across observers. See Cornsweet (1962) for a more general description of the staircase procedure.

2.9 Bootstrapping

Some of the parameters used to measure the observer's performance, such as the threshold and internal-to-external noise ratio, do not have a variance term associated with them. Since there were not enough observers used in these experiments to compute a mean across observers, bootstrapping was relied upon to provide an estimate of the dispersion associated with these measures of performance. Bootstrapping works by repeatedly selecting a subsample of the data and computing the mean of each subsample (Efron and Tibshirani, 1994). The variance of the resampled means is then used as an estimate of the variance associated with the parameter of interest.

2.10 Ideal Observer

To establish an upper bound on performance for this task, an ideal strategy is specified. This strategy has direct access to the signal information and is assumed to weight each pixel in the stimulus evenly. For this task, the ideal calculation is equivalent to cross correlating the stimulus and the signal template. This provides a measure of the similarity between the signal and the template, which is expressed by Equation (2.6) as the likelihood of a stimulus pixel (R_j) matching the corresponding template pixel (T_j). When the match is exact, $L(i) = 1$; as the dissimilarity between the stimulus and template increase the likelihood decreases exponentially. After computing the likelihood of each alternative, the ideal observer sums across the likelihoods leading to each response (in this case same or different) and combines them with the prior probabilities of each alternative occurring. The priors can be ignored in this case since both alternatives were

equally likely. A decision is then reached by choosing whichever response was more likely. As specified by specified by Tjan et al. (1995), the likelihood of the ith template is given by Equation (2.6) below, where the variance term σ^2 is the variance associated with the noise sample,

$$L(i) = exp\left[-\frac{1}{2\sigma^2} \sum_{j=1}^{N} (R_j - T_{ij})^2 \right] \tag{2.6}$$

The ideal strategy for this task can also be solved for directly by determining the optimal linear decision boundary. If the signals added to both intervals were the same, then the difference between the two intervals will result in noise. When the two signals are different, however, their difference will be twice the second harmonic. To separate responses that belong to the same category from responses that fall into the different category, a decision boundary can be established. Conveniently, the boundary that separates what is effectively the background from twice the second harmonic is simply the second harmonic. Following this approach, any response that, on average, falls above the second harmonic is classified as different, and any response falling below that boundary is judged to be a same response.

2.11 Equivalent Input Noise

As described in the previous chapter, noise masking can be used to investigate whether large threshold differences were associated with changes in the observers internal noise level or whether those differences were related to the observer's ability to extract the signal from the stimulus. The first possibility-differences in the internal noise level-refers to only the portion of internal noise that is invariant

with respect to the stimulus level. An estimate of the observer's contrast invariant internal noise is provided by the x-intercept of the noise-masking function. This is the value that would lead to a threshold of 0 if all of the contrast-invariant noise were removed from the system. The second point that determines the noise masking function is the slope parameter. Slope differences can result from a change in sampling efficiency, which is defined as the minimum proportion of energy necessary for an ideal observer to match the performance of the human observer (Tanner Jr and Birdsall, 1958). Legge et al. (1987) related the slope (k) and intercept parameters (N_i) to the external noise level (N_e) and contrast energy threshold (E) by equation (2.7) below.

$$E = k(N_i + N_e) \tag{2.7}$$

2.12 Response Consistency

Because both sampling efficiency and contrast-dependent noise depend on the level of signal, changes in both factors result in a change in the slope of the noise masking function. Therefore, a second estimate of the internal noise level is needed to determine if the total level of internal noise is influenced by the signal level. This estimate is provided using response consistency. This technique works by measuring the observer's responses twice using an identical sequence of external noise samples (Green, 1964; Spiegel and Green, 1981; Burgess and Colborne, 1988). This two-pass technique assumes that any differences between the first and second pass are due to internal noise. Evidence provided by Burgess and Colborne (1988) suggested that the total internal noise limiting the observer was

made up of a fixed contrast invariant component, as in Equation (2.7), and a second contrast dependent component, which Burgess and Colborne called induced internal noise. They determined that the level of induced noise was related to the signal energy (E) by the proportionality constant (m). The energy associated with an observer whose internal noise level depends on the external noise level can be expressed as follows (Gold et al., 2004):

$$E \equiv k(N + N_{eq} + m(N + N_{eq} + E)) \tag{2.8}$$

The contribution of induced noise can be measured by estimating the internal-to-external noise ratio (I/E) associated with an observer at multiple levels of external noise. Instability in this ratio reflects the influence of induced noise, and a significant change in the I/E ratio suggests that a single contrast-invariant noise source is inadequate to account for changes in the observers performance across multiple external noise levels. To estimate the I/E ratio, Burgess and Colborne (1988) plotted the covariation between percent agreement (PA) and percent correct (PC) from their two-pass procedure. Simulations were used to find the level of internal noise that, when added to the ideal observer, provided the best fit to the data. Gold et al. (2004) followed a similar approach, where simulations were used to estimate values of $k_{I/E}$ in Equation (2.9) that corresponded to various levels of internal noise added to the ideal observer,

$$PC = k_{I/E} \log_{10} \frac{PA}{100} + 100 \tag{2.9}$$

According to this relation, $k_{I/E}$ represents the slope of the line that relates PC and PA when PA is plotted on a log scale. Some hypothetical examples of

this relation are plotted in Figure (2.8) below.

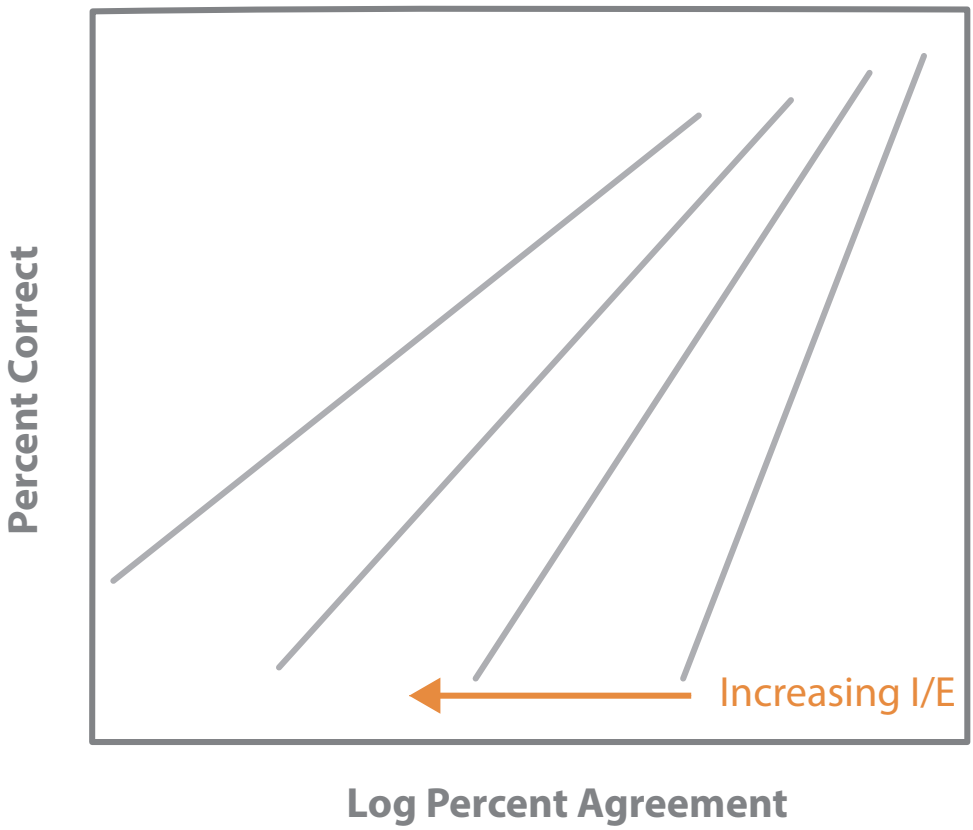

Figure 2.5: Response Consistency. The gray lines represent hypothetical correlations between percent correct and percent agreement. As the amount of internal noise increases the slope of the line decreases. The relationship between percent correct and percent agreement is made linear by plotting percent correct against percent agreement, as expressed by Equation (2.9) above. This indicates that a large increase or decrease in percent agreement leads to a small change in percent correct and vice versa.

The correspondence between the value of the slope parameter $k_{I/E}$ and the internal-to-external noise ratio is dependent on the task. To estimate this correspondence, a simulation of the ideal observer with various levels of internal noise was performed. A plot of the relation between I/E and $k_{I/E}$ is shown below in Figure (2.6) for the ideal observer performing three different tasks. The lines in

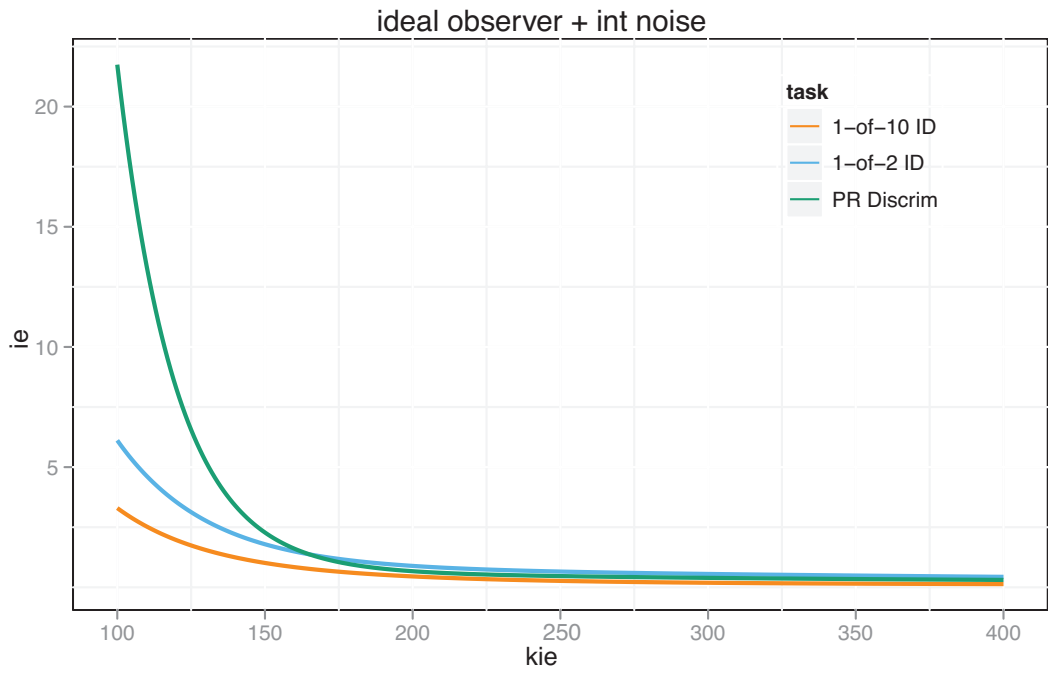

Figure 2.6: I/E estimates. This figure plots the relation between the slope obtained using response consistency and the corresponding I/E ratio for an ideal observer with internal noise performing three different tasks.

Figure (2.6) represent the best fits of a two term exponential function using the built-in MATLAB `fit` function, as specified by Gold et al. (2004),

$$I/E = \alpha + \gamma_1 e^{-\beta_1 k_{I/E}} + \gamma_2 e^{-\beta_2 k_{1/E}} \tag{2.10}$$

The tasks represented for by the lines are 1-of-2 identification, 1-of-10 identification, and the phase reversal (PR) discrimination task used in these experiments.

2.13 Calculation Efficiency

Originally applied to auditory signals, Beard and Ahumada Jr (1998) developed a method for identifying systematic patterns between the observer's re-

sponse and the noise added to the stimulus on each trial. This response classification technique works by averaging the noise samples associated with each stimulus-response pair over the course of the experiment. In a typical signal detection task, there are four possible stimulus-response pairs. These four outcomes ('Hit', 'False Alarm', 'Correct Rejection', 'Miss') are illustrated in Figure (2.7). They are the result of two possible responses ("Yes", "No") to the presence or absence of the signal. For the two-interval forced choice (2IFC) task used in these experiments, the mapping of stimuli and responses to these four outcomes is more complicated. The introduction of a second interval resulted in four additional outcomes as can be seen in the figure below.

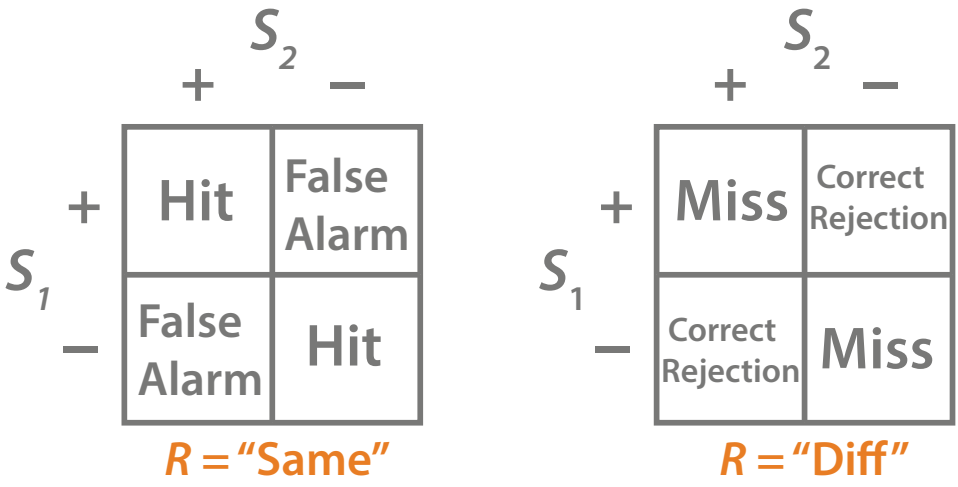

Figure 2.7: Stimulus–response outcomes. This figure helps relate the same-different task used in these experiments to a simple yes-no detection task. Since the task involved two stimulus intervals instead of one, as in the yes-no task, there were two stimulus combinations that led to each response. The rows identify the sign of the phase (positive or negative) that appeared in the first stimulus interval, and the columns indicate the sign of phase from the second interval. All of the outcomes from the 2x2 table on the right occur when a "Same" response was given, and the outcomes on the left result from a "Diff" response. The labels applied to the four different responses (Hit, Miss, etc) can then be used to combine noise samples into a classification image.

To specify a 2IFC task in terms of the four stimulus–response categories above, one response must be assigned to "Yes" and the other to "No". In these experiments, "Same" was equated with "Yes" and "Diff" with "No". Hence, a "Same" response when the stimuli that appeared were indeed the same resulted in a hit, and a "Same" response when the stimuli were different was a false alarm. Since there were two stimulus intervals, there were two different ways to achieve each of the four possible responses. A hit, for example, occurred when an observer responded "Same" to a pair of stimuli that were both in positive $(+,+)$ or negative phase $(-,-)$.

To compute a classification image, Ahumada (2002) simply averaged the noise samples that lead to each of the four possible responses, and then combined the averages according their response. That is, hits and false alarms both shared a "Yes" response so their averaged noise samples were added, and correct rejections and misses were combined since both resulted from a "No" response. The final step was to invert the "No" responses so that the final image was an estimate of the weights at each pixel in the image that led to a "Yes" response. Hence, the classification image (CI) that resulted can also be defined according to the following equation, where HIT, FA, etc, are the average noise fields associated with that response:

$$CI = (HIT + FA) - (CR + MISS) \tag{2.11}$$

For the present task, the calculation image can be computed using the same procedure. However, instead of four average noise fields, there were sixteen. This was because there were eight possible responses (given in Figure 2.7) and two noise samples associated with each response. The sixteen noise samples can be reduced to the four categories above by applying a weighting scheme where noise samples leading to a "Same" responses are each assigned a positive weight, and a negative weight is assigned to the "Diff" responses. In the simple case where there are only 4 noise samples, the classification image can be computed by taking the product of each of the four noise samples with the weights $[1, 1, -1, -1]$. For the same-different task, weights were assigned in the same way. When the stimuli were (+,+) and the response was "Same", the weights were $[1, 1]$. A "Same"

response to a $(-,-)$ pair of stimuli was weighted $[-1,-1]$, and the weighting of a "Same" response to a $(+,-)$ stimulus pair was $[1,-1]$. For a "Diff" response, all of the weightings were reversed. Since observers were limited to two responses, these weights can also be derived using a more generic framework introduced by Abbey and Eckstein (2002) for estimating classification images for 2–alternative forced choice (2AFC) tasks.

To help illustrate this process, the ideal observer was simulated for 100,000 trials of this same-different phase-reversal discrimination task and the average noise samples for each of the outcomes from Figure (2.7) were plotted. In the plot below, the averages associated with positive or "Same" responses are represented by solid lines and their negative counterparts by dashed lines. Interestingly, the incorrect responses (false alarms, misses) have larger amplitudes than the correct responses. This reflects a stronger influence of noise on incorrect responses. Since the ideal observer is not limited by internal noise, a mistake can only occur when the signal is disrupted by the noise in such a way that the noise resembles the incorrect alternative more than the correct one.

Figure (2.8) also shows that the outcomes associated with a Same response (hits, false alarms) are in phase, as are those associated with a Diff response (correct rejections, misses). Once the outcomes have been arranged in this way, all that remains is to combine them by negating or phase reversing those outcomes associated with a Diff response. The final outcome of this process is shown in Figure (2.9), and matches the actual signal quite closely. The weights that were used to compute the final classification image are as follows: [1 1 1 -1 -1 1 -1 -1

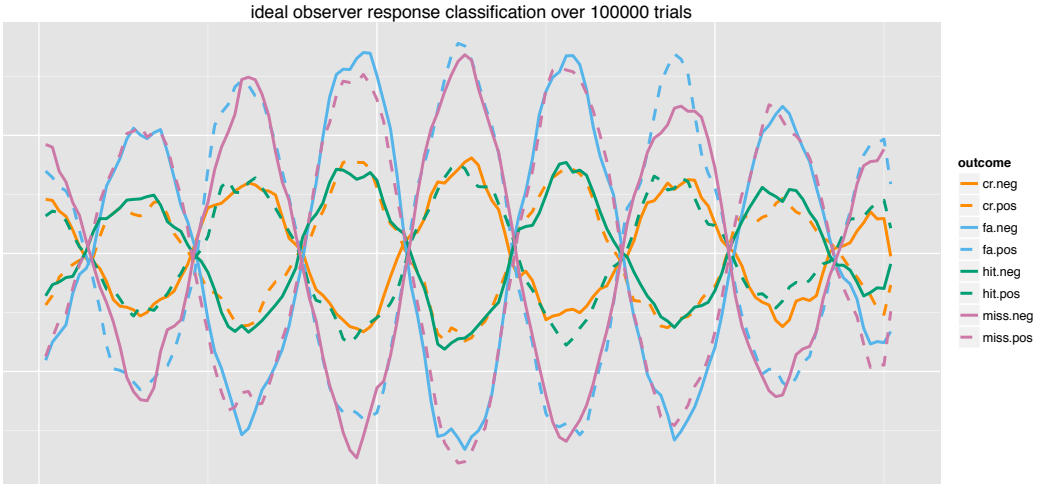

Figure 2.8: Simulated stimulus-response outcomes. These outcomes resulted from a simulated ideal observer. Solid and dashed lines represent positive and negative responses outcomes shown in 2.7. Positive outcomes are those associated with the first row of 2.7, and negative outcomes correspond to the second row. Prior to plotting, the lines were smoothed slightly by convolution with a [.7 1 .7] kernel.

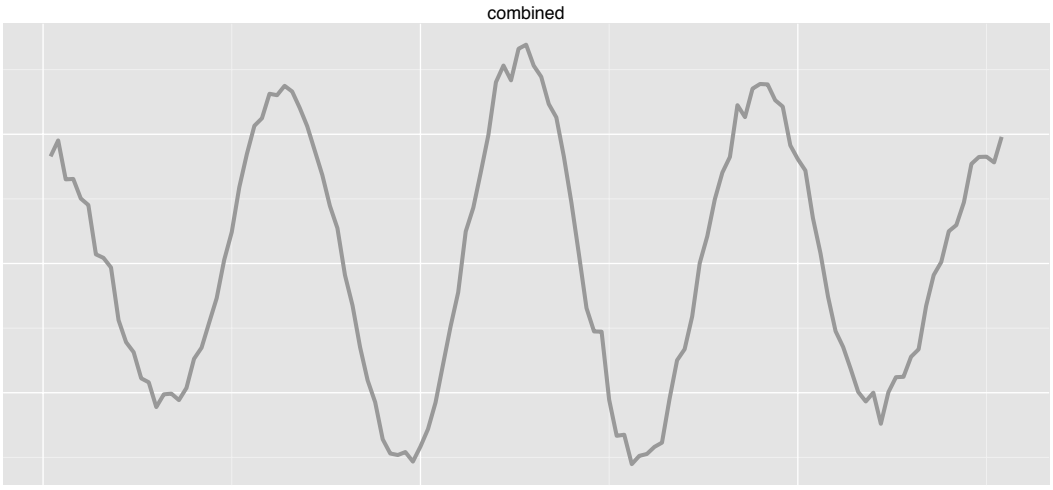

Figure 2.9: Simulated classification image. The eight possible outcomes from Figure (2.7) above were combined into a single classification image. After 100000 trials, the result closely matches the original signal.

-1 -1 -1 1 1 -1 1 1].

3 | Results

This chapter provides a detailed account of the experimental findings from four experiments. The goal of these experiments was to test two new possibilities to account for the findings of Bennett and Banks (1987) in which the observer's discrimination ability was drastically reduced by changing the spatial configuration of a pattern presented in the periphery. According to one alternative, observers were limited by an increase in the level of internal noise associated with judgments that relied on visual information that was shifted outside of the foveal region. This view is consistent with the assumption that observers relied on the same underlying template to perform discriminations across these two visual regions (Rovamo and Virsu, 1979; Rentschler and Treutwein, 1985). In Experiments 2 & 3, the level of internal noise was estimated using two separate methods to determine whether the phase relation of the signal pattern affected the internal noise level and whether the internal noise level depended on the level of external noise. A second alternative to account for the reduction in the discriminative ability of sine relative to cosine related patterns was that a fundamental shift occurred in the way the signal information was organized as a result of moving the stimulus from the fovea into the parafovea. This interpretation is consistent with a change in the observer's underlying template and may result in a shift in the observer's strategy from low to high eccentricity. Estimates of the observers'

templates for both the sine and cosine conditions at low and high eccentricities were provided in Experiment 4.

3.1 Experiment 1a: phase reversal detection

Part (a) of Experiment 1 was designed to determine whether there was any difference in the observer's ability to detect the sine and cosine patterns at high and low eccentricities. While detection of patterns that differed only in terms of phase was investigated for other compound grating patterns (Graham et al., 1978; Graham and Nachmias, 1971), this simple test did not appear to be mentioned in any of the previous experiments where this particular set of patterns was used. Hence, this experiment tests for the possibility that part of the difference in the observer's ability to discriminate between the two phase reversed patterns may have been due to one set of patterns being more easily detected than the other after external noise was introduced to the stimulus.

Unlike prior investigations, the signal patterns used in these experiments were embedded in a sample of external noise. To determine the influence of external noise on the observer's detection ability, detection thresholds were measured at a high and low level of external noise.

3.1.1 Methods

A simple modification to the experimental procedure used for phase reversal discrimination was made to produce a detection version of the experiment. Recall that the 2IFC phase reversal discrimination task (detailed in section 2.5) was for

the observer to determine whether the stimulus presented in the first interval was the same or different from the stimulus that followed in the second interval. For the detection version of the task, one member of the stimulus pair was replaced with a blank stimulus. This resulted in a 2IFC discrimination task where the observer was asked to discriminate between a single two-component grating pattern and a blank background.

Since this simple experiment was not considered until after the majority of data in the other experiments had already been collected, only one observer (s04) participated in this detection task. Thresholds for this observer were obtained for both the sine and cosine condition for stimuli presented centrally and at 5° of eccentricity. To determine the influence of the external noise level on detection ability, performance was measured at a high (nsd = $3.48e^{-6}$) and low (nsd = $6.26e^{-7}$) external noise level. These noise levels were selected to be as different as possible while insuring that the external noise was still visible. Hence, the lowest of the five noise levels was not used due to the possibility that there was increased spatial uncertainty at this noise level. RMS contrast thresholds were estimated in these 8 conditions (2 external noise levels x 2 phase relations x 2 eccentricities) by varying the contrast of both harmonics of the two-component grating pattern in a fixed 1:1 ratio across 250 trials.

3.1.2 Results

The detection thresholds presented in Figure (3.1) show only small differences in the detection ability of observer s04 in the sine and cosine condition in all but the foveal high noise condition. The minimal impact of phase on detectability in

these conditions is consistent with previous findings that the phase relation was not a factor in the detectability of a compound grating (Graham and Nachmias, 1971; Graham et al., 1978). However, when the noise level was increased in the fovea, the threshold in the sine condition was 1.9 times greater than in the cosine condition. To provide some indication of the significance of this difference, the sine threshold, which was estimated to have a greater variance than the cosine threshold, was 2.75 standard deviations larger than the cosine threshold. This disparity suggests that there was a noticeable difference in the detectability of the two patterns in the high noise condition.

The effect of shifting the stimulus presentation from 0° to 5° of eccentricity can be seen by comparing the left and right panels of Figure (3.1) below. Interestingly, the effect of eccentricity was more noticeable in the low than high noise condition. This interaction between eccentricity and noise level will be discussed in more detail in Experiment 1c.

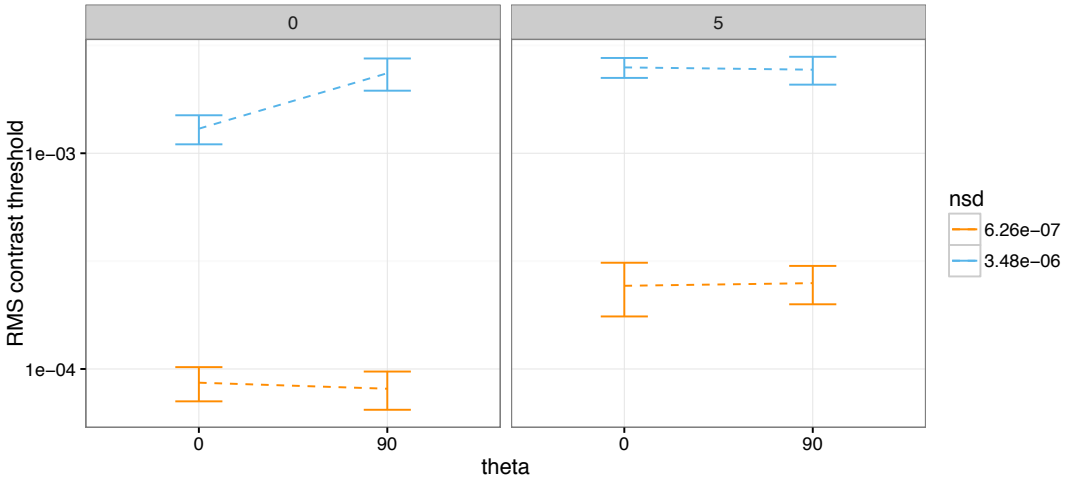

Figure 3.1: Phase detection results. RMS contrast thresholds are plotted on a log scale as a function of phase angle (0 or 90°). A lower threshold indicates that the observer required less contrast to achieve a level of performance of 71% correct. The colors (orange and blue) indicate the level (low and high) of external noise. Results from the 0 eccentricity (foveal) condition are shown in the left panel and the 5° eccentricity condition is shown on the right–as indicated by the labels on the top of the panels. Errorbars extended to ± 1 standard deviation of threshold estimated using 1000 iterations of a bootstrapping procedure.

3.2 Experiment 1b: naive observer phase reversal discrimination

To verify that the difficulty discriminating sine patterns in the periphery reported by Bennett and Banks (1987) was not limited to the small set of trained observers used in their experiments, a pilot experiment was conducted using volunteers recruited from the undergraduate subject pool. This sample of observers was used to determine the extent to which the deficiency in discriminating sine related patterns was characteristic of untrained observers from the general population. Since previous experiments did not involve the use of external noise, another goal of this experiment was to test whether sine related discriminations

remained problematic when viewed at high eccentricities after the signal pattern had been corrupted by external noise.

3.2.1 Observers

Sixty students from the undergraduate psychology subject pool participated in this experiment. These subjects were unfamiliar with the stimulus patterns used in the experiment and had no prior experience with the experimental procedure. All of the subjects gave informed consent and received course credit in exchange for their participation. In order to participate in the experiment, subjects were required to have normal or corrected-to-normal visual acuity (self-reported). Of the 60 observers that participated in these experiments, thresholds from only 37 observers could be reliably estimated; in some cases observers performed better in the high eccentricity than the 0 eccentricity condition, suggesting that observers were not following instructions and shifting their eyes to the center of the stimulus in the high eccentricity condition. In other cases observers were simply unable to perform the task in the high eccentricity condition. Consequently, data from a large portion of the observers (23) were excluded from the analysis presented below.

3.2.2 Methods

To determine the effects of eccentricity and phase on untrained observers when signals were embedded in external noise, RMS contrast thresholds were estimated using the phase reversal discrimination task described in Section (2.5) for stimuli presented in the fovea and at either 3 or 5 degrees eccentricity in both the sine and cosine condition. Initially, observers were tested at 5-degrees in the high

eccentricity condition; however, due to poor performance at this eccentricity, presentations were shifted inwards to 3 degrees to make the task more manageable for observers. Of the 37 whose results were included in analysis, 14 viewed the stimuli at a 5-degree eccentricity. The RMS contrast of the entire grating pattern (i.e., both components) was varied to obtain a threshold across 250 trials in each condition. The external noise level was fixed at the highest level (nsd = $3.48e^{-6}$) to determine the full effect of external noise.

Participants in this experiment were instructed to judge whether the stimuli presented in the first and second interval were the same or different. Prior to each experimental block, which consisted of 250 trials, observers were given a practice block consisting of 12 trials in which feedback was provided after each trial. At the beginning of the practice block, the stimulus presentation was extended and the noise level was lowered to allow the observer to clearly see the signal pattern. When the stimulus presentation was shifted from the center of screen to an eccentricity of 3 or 5°, the observer was instructed to continue looking at the center of the screen for the duration of the trial. To draw attention to the center, the fixation cross flickered before the the stimulus appeared and remained present in the center of the screen throughout the stimulus onset. Since the task was less difficult when the stimuli were presented in the center of the screen, the 0° eccentricity condition always preceded the higher eccentricity condition in both the sine and cosine conditions. While this constraint introduced a possible order effect, it also ensured a more conservative estimate of the effect of eccentricity since any learning effects would only serve to reduce thresholds in the higher eccentricity condition.

3.2.3 Results

The results from the 37 observers whose thresholds could be reliably estimated are shown in Figure (3.2). The relative performance between the cosine and sine condition can be judged by comparing the orange and blue boxplots. These boxplots represent the distribution of the thresholds in the two conditions; the growing size of the blue box in the sine condition indicates larger variability in the threshold estimated from that condition. The median across all of the observers, pictured as the solid bar within each of the boxes, tended to be slightly higher in the sine than the cosine condition. The effect of eccentricity, which can be seen by comparing the boxes from left to right, does not indicate a consistent increase in the sine relative to the cosine condition. However, there did appear to be an overall trend in which the sine condition was more difficult than the cosine condition.

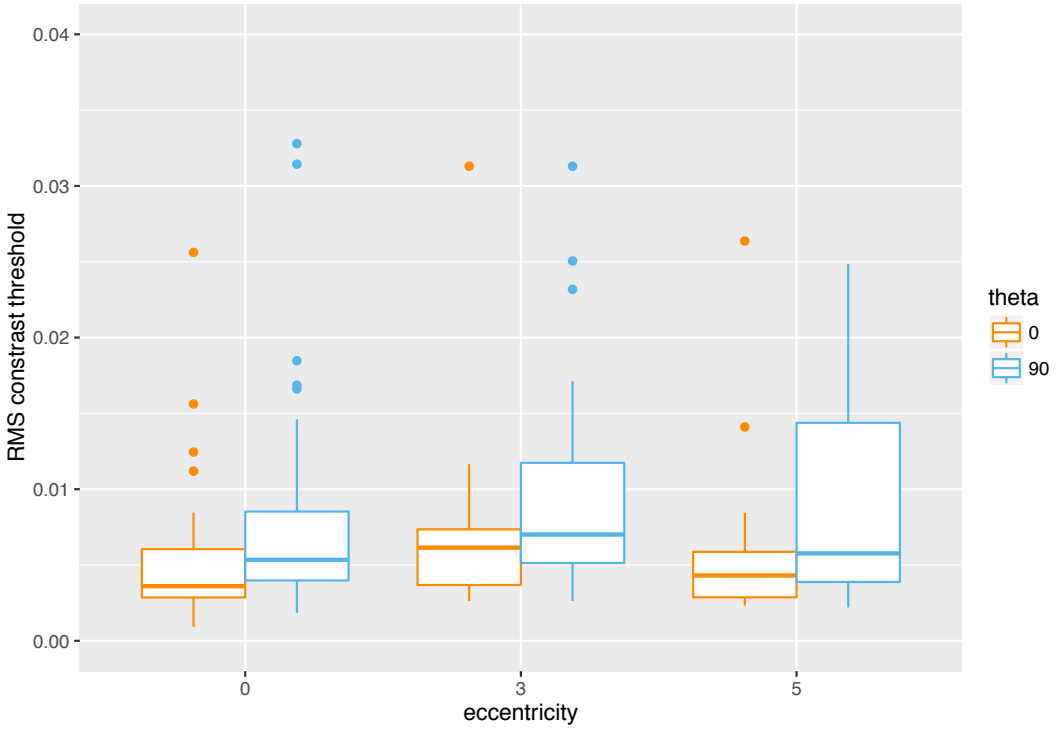

Figure 3.2: Effect of cosine vs sine on untrained observers. Contrast thresholds from each of the 37 observers represented by boxplots. All 37 observers are represented in the 0 eccentricity condition, a subset of the observers contributed to the boxplots in the 3 and 5° conditions. The boxplots cover the 1.5 times the inter-quartile range of the thresholds (i.e., 25^{th} to 75^{th} percentiles) and outliers are shown as the points beyond this range. The phase relation, 0 for cosine and 90 for sine, is indicated by the legend, and the eccentricity in degrees of visual angle is presented on the x-axis.

The results above provide clear evidence that naive observers could not be relied on to carry out the remainder of the experiments. Naive observers had difficulty following instructions, particularly in the high eccentricity condition. Results from a number of these observers suggested that they were moving their eyes to look directly at the stimuli in this condition. Another issue that arose was that a subset of naive observers were simply unable to perform the task in the high eccentricity condition, perhaps because they were unclear about what the signal pattern looked like. Overall, there was simply too much variability

in the performance of these observers to provide reliable threshold estimates. As a result, a small number of trained observers were used in the remaining experiments. These observers were trained in pilot experiments to gain familiarity with the task and stimuli. A subset of these observers also performed a large number of trials to estimate perceptual templates in Experiment 4.

3.3 Experiment 2: Noise Masking

One possible account for the accelerated loss of spatial position sensitivity associated with sine related phase information reported by Bennett and Banks (1987) is that observers experienced higher levels of internal variability when viewing the sine stimuli than the cosine stimuli. If the enhanced difficultly performing discriminations within the sine channel was the result of increased contrast-invariant internal noise, then we would expect to find a greater negative x-intercept in a noise masking function measure for sine relative to cosine phase reversal discriminations. A second possibility is that observers may have been less efficient at extracting the signal in the sine than the cosine condition, which would produce a change in the slope of the noise masking function. To determine which of these two possibilities was more likely, noise masking functions were measured for a set of four trained observers in this experiment.

3.3.1 Observers

The data obtained in this experiment were collected from four observers. These observers all had some prior experience with psychophysical experiments

and participated in pilot experiments to familiarize themselves with the task and stimuli. The following unique identifiers were assigned to the four observers: s04, s10, s14, s21. One observer (s04) participated in several rounds of pilot experiments. The other three observers were compensated $10/hr for their participation. All of the observers had normal or corrected-to-normal visual acuity; s04 and s10 were emmetropes and therefore did not require any form of visual correction; s14 wore glasses while participating, and s21 wore contact lenses.

3.3.2 Methods

The stimuli and task used in this experiment were described in Sections 2.4 and 2.5 of the previous chapter. The signal was formed by a fundamental, which was always in cosine phase, and second harmonic in either sine or cosine phase. The sign of the second harmonic was flipped to create a "sine" and "cosine" pair of stimulus patterns. The frequency of the fundamental was 2 cycles/image, and the amplitudes of both the fundamental and second harmonic were varied in a fixed 1:1 ratio according to a staircase procedure (see Section 2.9) in order to obtain a threshold estimate. All four observers viewed the stimuli centrally and at least one a higher eccentricity. An eccentricity of 0 degrees corresponded to a presentation of the stimulus in the center of the visual field. During pilot experiments, the effect of increasing eccentricity was different for each of the four observers. For example, shifting the stimulus position by as little as 2° resulted in a noticeable effect of phase for one observer but not the others, and by 5° some observers were unable to reliably perform the task. Hence, the results of based on pilot experiments, the higher eccentricity for each observer was tailored to be a point where the task could still be reliably performed and a clear distinction

could be made between performance in the sine and cosine condition. Similar variability in the effect of eccentricity on different observers was also evident in the experiments of Levi and Klein (2002).

As in the previous experiment, the task was to discriminate whether the two stimuli, presented one after the other, were the same or different. The duration of each stimulus onset was 250 ms. A different sample of Gaussian white noise was added to the signal on each trial to form the stimulus. To measure a noise masking function, the observer's RMS contrast threshold was measured across five external noise spectral density levels ($3.48e^{-7}$, $6.26e^{-}7$, $1.11e^{-6}$, $1.95e^{-6}$, $3.48e^{-6}$).

To limit any order effects, two of the four observers were assigned to perform the cosine condition first and the other two started with the sine condition. Within the sine and cosine conditions, the level of external noise used in each block of 250 trials was randomly selected for each observer. This was done to minimize any confusion about which set of the stimuli the observer had been asked to discriminate.

In addition to estimating a noise masking function, the thresholds from the lowest external noise level were also used to verify that the results of Bennett and Banks (1987) could be replicated on this small set of trained observers. Other than introducing a small level of external noise noise, Bennett & Banks measured thresholds by adjusting the contrast of the second harmonic relative to a fixed contrast fundamental. The effect of modifying the relative contribution of the second harmonic by a staircase procedure was to slightly change the appearance

of the patterns at each step in the staircase. Since the experiments in this thesis were restricted to a single template of the underlying signal, thresholds were measured by varying the contrast of both the fundamental and second harmonic in equal proportion. Another difference between this protocol and the one used by Bennett & Banks was that RMS contrast (defined in Section 2.6) was used instead of Michelson contrast. Considering that these two measures of contrast could not be directly related (Peli, 1990), this comparison was reported in terms of the ratio of the RMS contrast thresholds in the sine to cosine condition—i.e., the odd-even ratio.

3.3.3 Results

To determine if the results obtained from this new set of trained observers were consistent with the findings of Bennett and Banks (1987), the odd-even ratios from the lowest noise condition were compared to the odd-even ratios provided by Bennett & Banks in Figure (3.3) below.

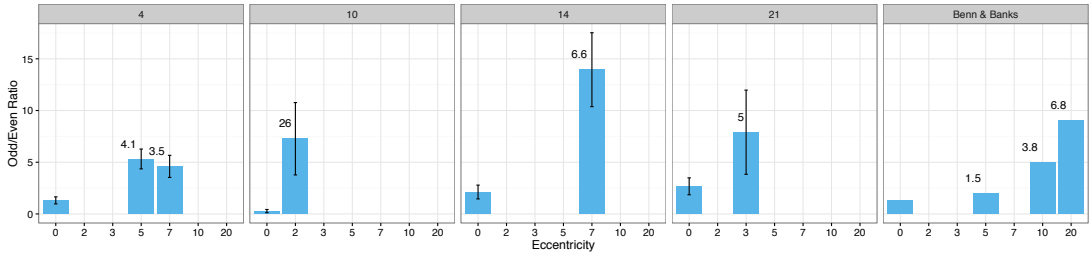

Figure 3.3: Odd-even ratios for the four observers in this experiment compared to the averages obtained by Bennett & Banks across a range of eccentricities. Stimuli were presented to each observer in the fovea, which corresponded to an eccentricity of 0 degrees, and at one, or in the case of observer 4, two higher eccentricities (expressed in degrees of visual angle). A separate panel is shown for each of the four observers and for the results of Bennett and Banks (1987) with corresponding labels above each panel. The heights of the bars indicate the observers odd-even ratio—the ratio of the observer's threshold in the sine condition to their threshold in the cosine condition at the lowest noise level. Ratios larger than 1 indicate that the observer performed worse in the sine than the cosine condition. The number shown above the bar corresponding to the higher eccentricity displays the ratio of the high to low eccentricity odd-even ratio. The errorbars extend to $\pm$ 1 the standard deviation of the odd-even ratio, which was computed by taking the variance of a ratio and assuming the thresholds (m_O, m_E) were uncorrelated as follows: $\sigma_{O/E} = \sqrt{\left(\frac{\sigma_O}{m_O}\right)^2 + \left(\frac{\sigma_E}{m_E}\right)^2}$

The odd-even ratios plotted in this figure are defined as each observer's RMS contrast threshold in the sine condition as a proportion of their threshold from the cosine condition. To limit any potential effects due to the presence of noise, the odd-even ratios shown in Figure (3.3) are from the lowest noise condition. In this condition, observers reported that the noise was near or below visible levels, which is similar to experiments of Bennett & Banks where stimuli were presented without external noise. While there was more variability across observers as eccentricity increased, the increase in the odd-even ratio in the presence of external noise appears to be qualitatively consistent with the findings of Bennett and Banks (1987). Overall, the odd-even ratio tended to increase even more dramatically for the observers in this experiment than in the experiments reported by

Bennett and Banks (1987), possibly due to the presence of external noise.

Given that the disparity in the discrimination ability of sine and cosine related patterns at high eccentricity could be reproduced on a small set of trained observers, the next step was to estimate how this disparity was reflected in terms of the two potential factors limiting the observer's performance—i.e., contrast-invariant internal noise and sampling efficiency. In this experiment, noise masking was used to provide an estimate of the slope and negative x-intercept of the observer's noise masking function. Changes in these values can be used to identify which of these two limitations (internal noise or sampling efficiency) was more likely to be associated with the decline in performance in the sine condition at high eccentricity. Another goal of this experiment was to ensure that raising the level of external noise did not alter the overall similarity in performance between these experiments and those reported by Bennett and Banks (1987).

To verify that increasing the external noise level did not alter the odd-even ratio, the dot plots in Figure (3.4) below show the range of performance across all five levels of external noise for each of the four observers. Based on a visual inspection of Figure (3.4), the level of external noise did not appear to be directly related to the odd-even threshold ratio. On average, odd-even ratios in the higher eccentricity condition(s) increased relative to the foveal condition.

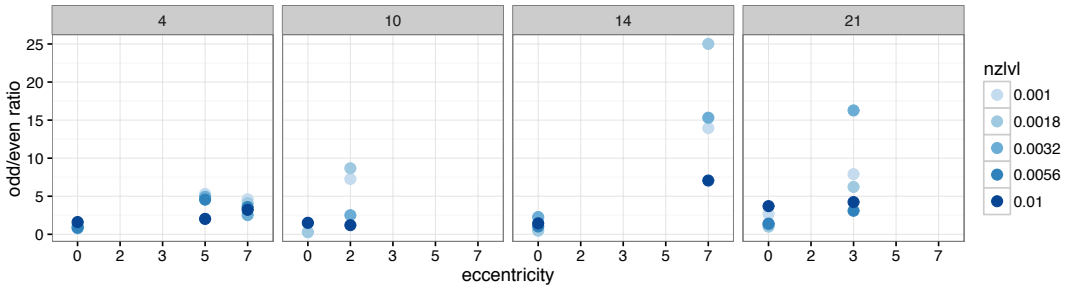

Figure 3.4: Effect of external noise level on odd-even ratio. Odd-even ratios are plotted for each observer to show the effect of varying the external noise level from low to high (light blue to dark blue). Eccentricity (reported in degrees of visual angle) increased along the x-axis.

For observers that showed considerable variability across external noise levels, the highest level of external noise was associated with a relatively small odd-even ratio, and the largest odd-even ratios corresponded to mid-level external noise. This trend, along with the results of the detection experiment from the high noise condition, suggested that there might have been a change in the observer's strategy at different external noise levels. That is, due to a change in the external noise, the observer may not have been able to rely on the same portions of the signal to reliably perform the task. In the sine condition, for example, the most discriminative regions of the signal, which corresponded to the zero crossings of the luminance profile, may have been more difficult to locate at higher noise levels. Evidence for systematic differences in the observer's use of spatial frequency at different levels of external noise was provided by Abbey and Eckstein (2009). These authors found that at low noise levels observers adopted a strategy in which they preferred less-informative, lower-frequency components of the signal over more-informative, higher-frequency components. They also found that raising the external noise level could decrease this bias toward different portions of the

amplitude spectrum. To provide a better understanding of how performance varied with the external noise level, noise masking functions were examined in the next section.

3.3.3.1 Noise Masking Functions

Noise masking functions from each of the four observers are shown in Figure (3.5). Both the thresholds (shown in RMS contrast units) and noise spectral density (nsd) are plotted in linear coordinates. The panels are labeled according to the observer (gray label above) and eccentricity (gray label below). The irregularities in the noise masking function, particularly at low noise levels, result in a shape that differs from the typical linear fit in which thresholds increase in direct proportion to the external noise level. In general, thresholds at lower noise levels appeared to be overestimated by the regression line while high noise thresholds tended to be underestimated. This pattern (the details of which are analyzed in Figure 3.7) indicates that, at least for a portion of the noise masking function, the effect of external noise was not consistent across the two regions of the visual field. One potential explanation for this unusual finding is that the external level was not raised to a sufficiently high level, and therefore the noise masking functions plotted are only the beginning part of the entire function. Another possibility is that, consistent with Abbey and Eckstein (2009), observers may have used different portions of the signal depending of the level of external noise and eccentricity. Regardless of the details of these interactions, the shape of the noise masking functions indicated thresholds for some observers were not well described by a linear fit to the data. Consequently, the intercept and slope parameters associated with the noise masking function, which will be discussed

in more detail below, are difficult to interpret due to inconsistencies in these observers' responses across external noise levels.

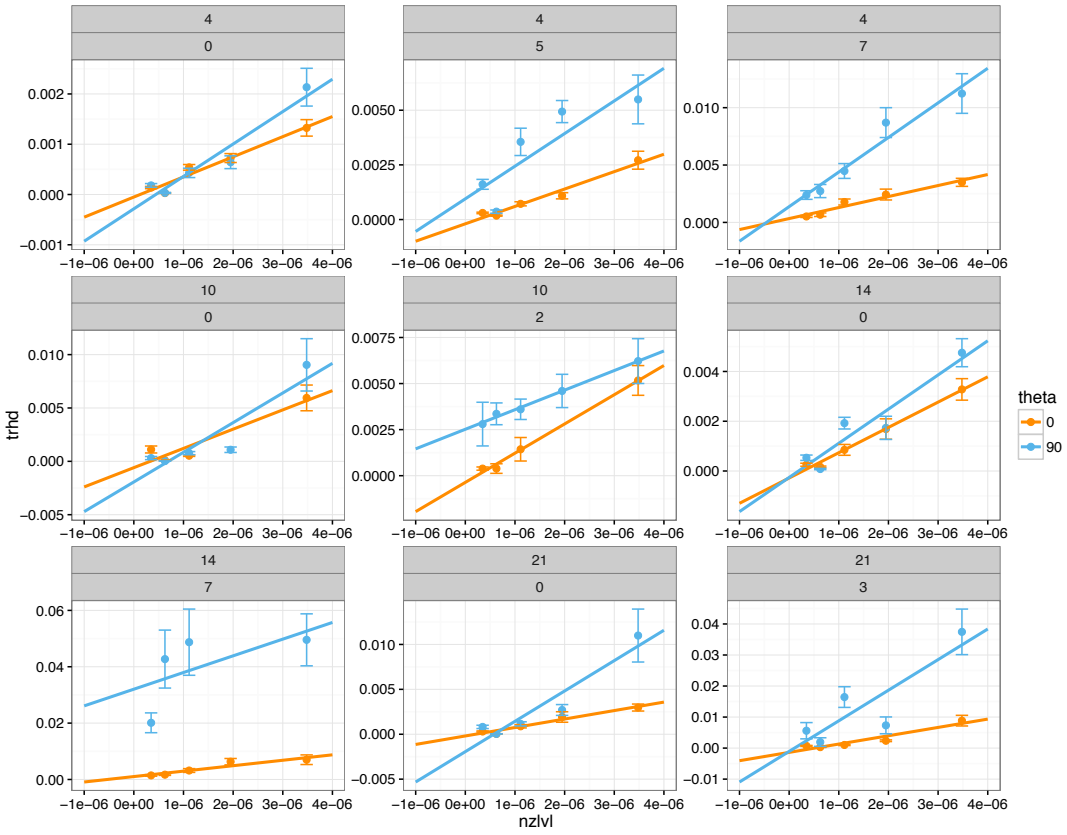

Figure 3.5: Experimental noise masking functions. These plots show the relation between the observer's RMS contrast threshold (y-axis) and the external noise spectral density (x-axis), both on a linear scale. The gray-shaded label on the top of each panel indicates which of the four observers (4, 10, 14, 21) contributed the data. The eccentricity (in degrees of visual angle) is provided in the second row. The five data points correspond to each of the five noise levels, provided that the threshold estimate was reliable. Error bars extend to one standard deviation above and below the observer's threshold. The blue and orange lines are fitted linear regression lines; the color indicates whether the stimulus pair was in cosine phase (orange) or sine phase (blue).

One interesting pattern that emerged across observers was that thresholds in the lowest noise condition were typically higher than thresholds in the second lowest noise condition. This surprising improvement in performance at a higher

external noise level may have been due to a reduction in spatial uncertainly. More specifically, if the noise were below the observer's detection threshold in the lowest noise condition the observer may have experienced some uncertainty over the exact location of the stimulus presentation; however, when the external noise was clearly visible, the outline of the stimulus may have reduced some spatial uncertainty about the position of the stimulus and lead to an improvement in performance.

To examine how, on average, thresholds changed as the external noise level was raised from one level to the next, the proportional differences in thresholds between consecutive noise levels are plotted in Figure 3.6 below. These changes in threshold were computed by taking the ratio of each threshold to the threshold at the previous noise level. The color of the bar indicates whether the stimuli were presented in the fovea (low) or at a higher eccentricity (high). The trends in the left and right panels, which are separated based on the phase relation of the signal, do not appear to be remarkably different. In both panels, larger sequential differences appear in the low than in the high eccentricity condition.

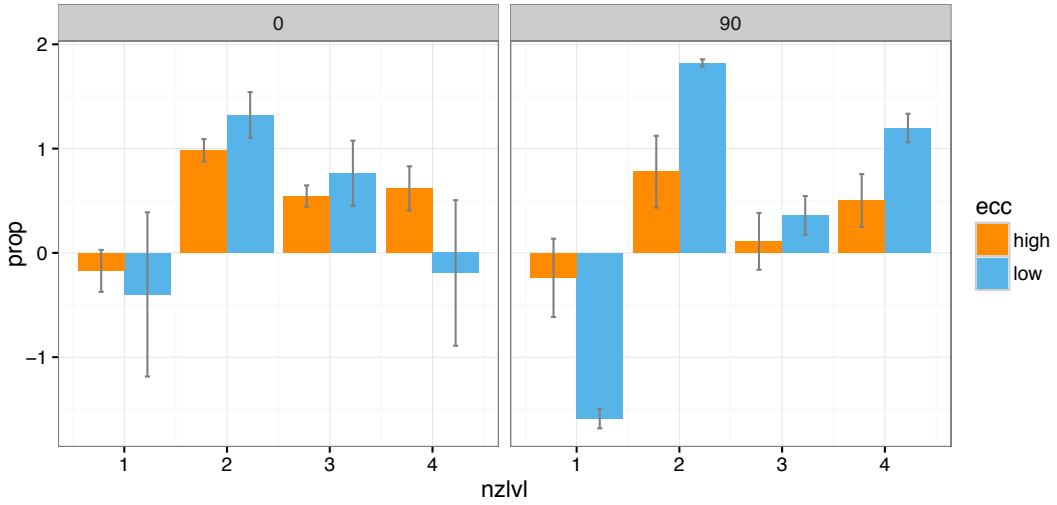

Figure 3.6: Proportional threshold differences across external noise levels. This plot shows changes in the observers threshold as a proportion of the previous threshold across external noise levels. Since thresholds were measured at 5 levels of external noise, four proportional differences were calculated. The color indicates whether the thresholds were measured in the low or high eccentricity condition. The low eccentricity was always 0 degrees of visual angle and the high eccentricity ranged between 2-7 degrees of visual angle depending on the observer. Error bars extend to $\pm$ 1 standard error of the mean.

For completeness, the slope and intercept values associated with these linear fits were examined in more detail in next set of figures. While these parameters are difficult to interpret on their own due to non-linearities in the noise masking functions, they are still useful for comparing how these observers differed between the sine and cosine condition in terms of the two broad classes of limitations.

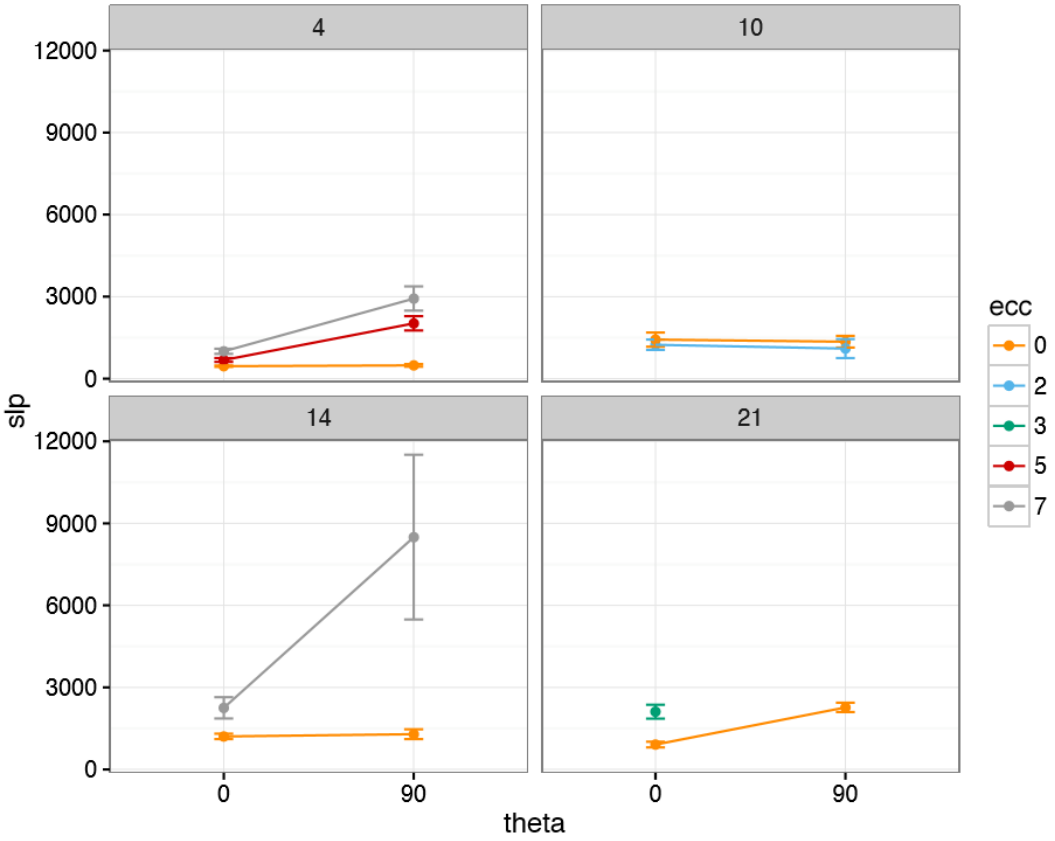
4
10
14
21
12000
9000
6000
3000
0
slp
0
90
theta
ecc
0
2
3
5
7

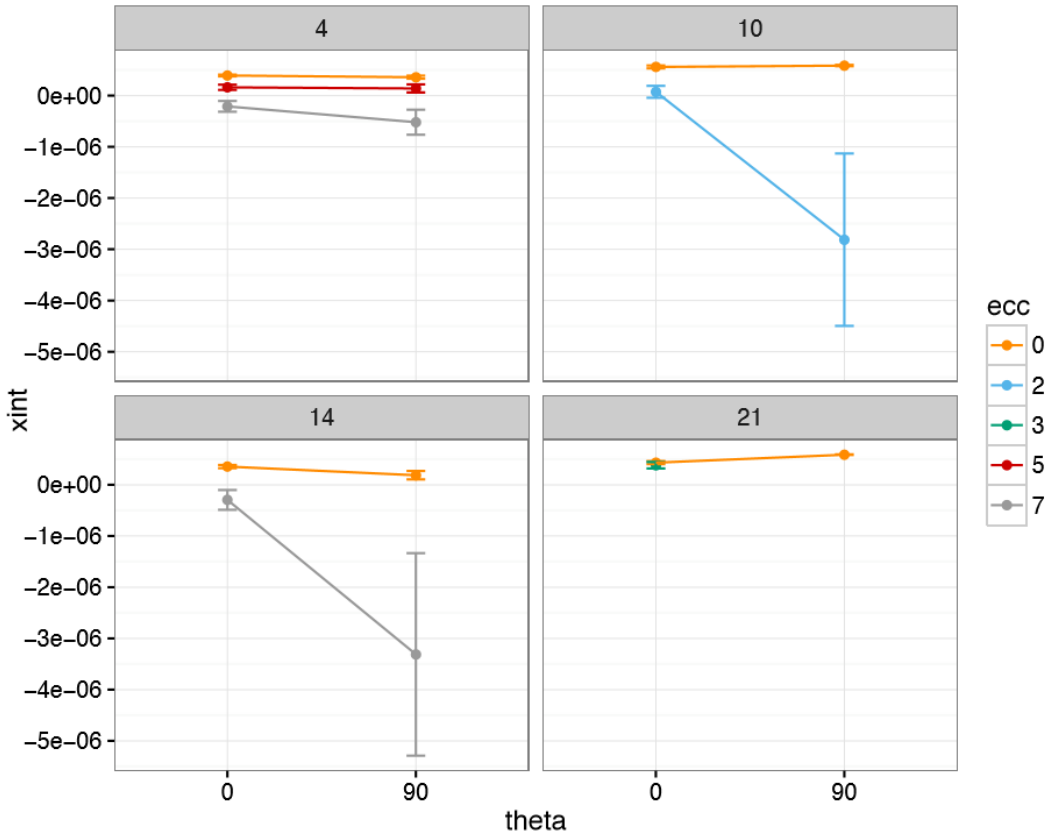

Figure 3.7: Slope and x-intercept of the noise masking functions. The slopes of the noise masking functions (Figure 3.5) from each of the four observers are shown in the top panel. The lines connecting the slope from the cosine (0) and sine (90) condition indicate the influence of phase on the shape of the noise masking function. In the bottom panel the negative x-intercept from the linear fit to the noise masking function is presented. The lines in both panels were colored according to the eccentricity of the stimulus presentations, and the panels were separated by observer. The errorbars extend to $\pm$ 1 standard deviation of the slope and negative x-intercept. A bootstrapping procedure in which a subset of the data were resampled 1500 times was used to provide an estimate of the standard deviation.

In Figure (3.7) above, the slopes and negative x-intercepts from the linear fits of the noise masking functions are plotted. The panels are separated and labeled by observer and the lines are colored according to the eccentricity (in degrees of visual angle) of the stimulus presentations. Due to unreliable threshold

estimates, one of the fits from the bottom right panel was excluded. Also note that in some cases, the x-intercept was actually positive, which is theoretically impossible because it implies that, when the external noise level is removed, the observer would actually have a negative threshold.

Based on Figure (3.7) above, there did not appear to be an overall pattern in the slopes and intercepts across all four observers. For example, observers 4 and 21 (for the available data) had larger differences in slope than x-intercept, whereas observer 10 had larger differences in the x-intercept than the slope, and finally observer 14 had large differences in both parameters. However, as noted above, the differences in slope and x-intercept, which were more pronounced in the sine condition, were difficult to interpret due to the irregularities in the shape of the noise masking. Consequently, changes in the x-intercept and slope parameters could not be relied upon to draw conclusions about the factors limiting performance in the sine condition.

3.3.3.2 ANOVA

In Experiment 2, the effects of the phase relation, eccentricity of the stimulus presentation, and the external noise level on the observer's RMS contrast threshold were all measured. The results of this experiment showed that changing the levels of each of these three factors affected the observer's threshold. Raising the level of external noise made the task more difficult; consequently, the observer required a higher signal contrast to perform the discriminations. Similarly, presenting the stimulus at a high eccentricity also impaired the observer's ability to perform the discriminations. The effect of phase (i.e., whether the patterns were

formed by a second harmonic in a sine or cosine phase) appeared to depend on whether the stimuli were presented at high or low eccentricities. Thus far, these interpretations have been formed mainly by visual inspection of the experimental data. To determine if these findings were also consistent with statistical inferences made based on the proportion of variance in the observer's RMS contrast threshold accounted for by each factor alone or in combination with other factors, an ANOVA was performed. Since all of the factors were expected to have an effect on the observer's threshold, a full ANOVA was tested, which included all of the interaction terms. Additional variance terms were also included to account for the individual variability contributed by each observer.

	DF	Sum Sq	Mean Sq	F	Pr(>F)
Theta	1	$7.5e^{-4}$	$7.5e^{-4}$	11.7	0.002
NSD	4	$6.9e^{-4}$	$1.7e^{-4}$	2.7	0.046
Ecc	4	$1.6e^{-3}$	$4.2e^{-4}$	6.6	0.0004
NSD:Theta	4	$1.6e^{-4}$	$4.2e^{-5}$	0.66	0.62
Theta:Ecc	4	$1.1e^{-3}$	$2.7e^{-4}$	4.36	0.005
NSD:Ecc	16	$4.7e^{-4}$	$2.9e^{-5}$	0.46	0.95
NSD:Theta:Ecc	15	$3.3e^{-4}$	$2.2e^{-5}$	0.35	0.98
Residuals	37	$2.4e^{-3}$	$6.03e^{-5}$		

Table 3.1: Contrast Threshold ANOVA. The full ANOVA was conducted for the effects external noise, phase, and eccentricity on the observers contrast threshold. A random effect term was included in the model to account for the additional within subject variability introduced by the four observers. In this experiment there were 5 levels of NSD, 2 levels of Theta, 5 levels of eccentricity (split among observers), and 4 observers.

Based on Table (3.1) above each of the factors that were manipulated in the

experiment: external noise level (NSD), phase (Theta), and eccentricity (Ecc) had significant main effects on the observer's threshold at the $\alpha = .05$ level, however there was also a significant interaction between phase and eccentricity. The absence of an interaction between external noise and eccentricity suggested that the effect of external noise in the fovea was not different from the effect of external noise in the parafovea. Some evidence for such an interaction did appear in the noise masking functions where there was under fitting at low eccentricity and over fitting at high eccentricity. However, the overall impact of these differences was not statistically significant. Similarly, the lack of an interaction between external noise and phase can be taken as evidence that the effect of noise was not different in the sine and cosine conditions. Overall, the results of this ANOVA provide reassurance that the experimental effects of the independent variables are consistent with the effects phase and eccentricity observed by Bennett and Banks (1987), and that the introduction of external noise did not introduce interactions with the other experimental variables. That is, from the table below the conclusion can be drawn that there was a main effect of external noise on the observer's threshold and an interaction between eccentricity and phase, as expected.

3.3.3.3 Psychometric Functions

Other clues about how the observer was impacted by changing the phase relation of the signal pattern can found by exploring the psychometric functions. In addition to providing an estimate of the observer's threshold, the slope of the psychometric function provides some indication of the uncertainty associated with the threshold estimate. In particular, a steeper slope implies that the observer

was able to achieve a higher level of performance with a small increase in signal contrast; whereas, a shallower slope indicates that there was more uncertainly about where to place the observer's threshold because a larger increase in contrast was required to improve performance.

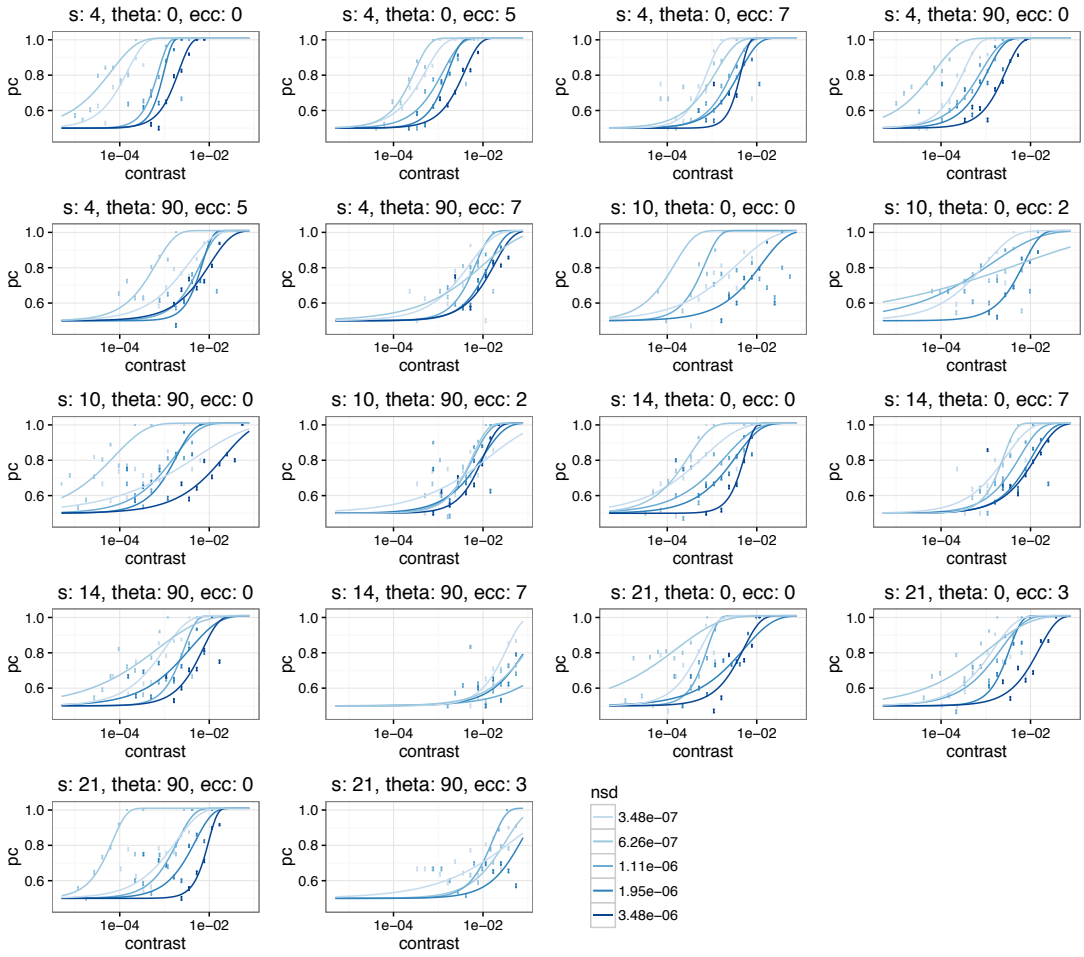

Figure 3.8: Psychometric Functions. In each panel, the lines show the fit of a Weibull distribution to the average percent correct (y-axis) at each RMS contrast level (x-axis) for each of the five levels of external noise. The lines are colored according to the external noise level: higher external noise levels corresponded to darker shades of blue and lower levels to lighter shades of blue. The error bars indicate the standard errors associated with each contrast level. In the title of each figure, 's' corresponds to the subject or observer, 'theta' is the phase relation (0 or 90 degrees) and 'ecc' indicates the eccentricity (0, 2, 3, 5, or 7 degrees of visual angle). Not all panels contain all five levels of external noise, those with missing levels were omitted due to unreliable threshold estimates.

To assess the reliability of the threshold estimates, psychometric functions for each combination of observer, eccentricity, and phase relation are shown in Figure (3.8) above. The relation between RMS contrast (x-axis) and percent correct

(y-axis) was fit to a Weibull distribution (see section 2.3 for details) to generate a psychometric function. If the level of internal noise were fixed across all five levels of external noise, then the slope of the psychometric function would remain constant and the five psychometric functions would be neatly ordered from left to right according to the external noise level. For example, in the panel labeled 's: 4, theta: 0, ecc: 5' the psychometric functions follow a similar shape, and the steep portions of the functions are ordered by external noise level. Other panels, however, such as those from 's: 10', display considerable differences in the shape and order of the psychometric functions.

Comparisons based on the relative position of the fitted functions tend to confirm the finding that thresholds in the sine condition ('theta: 90') were greater (shifted to the right) than those in the cosine condition ('theta: 0'), and this disparity grew as eccentricity increased. When the shape of the fits is also taken into account, the increasing disparity between sine and cosine is also accompanied by increased uncertainty (i.e., shallower slopes) in the sine condition. In Figure (3.9) below, aggregate changes in the slope of the psychometric functions across observers and eccentricities are represented as boxplots. This figure shows a small overall increase in both the slope and the variability associated with the slopes as the external noise level increases in both conditions. Based on this figure, slopes in the cosine condition also tend to be higher than those in the sine condition.

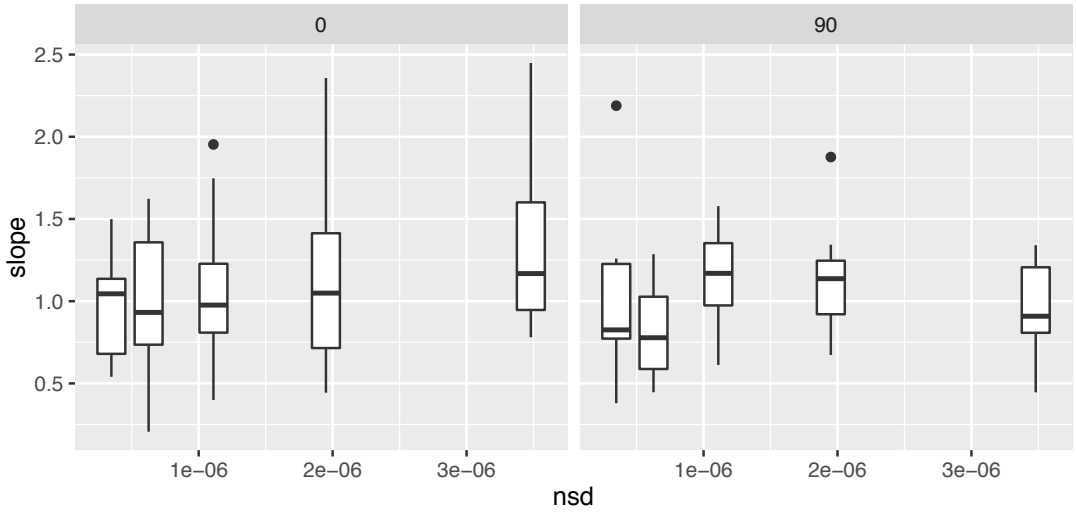

Figure 3.9: Boxplots containing slopes of the psychometric functions from all four observers shown in Figure (3.8) are shown for both the cosine and sine condition (left and right panels) across all five levels of external noise. Slopes from the foveal and higher eccentricity condition are combined into each boxplot. The height of the box corresponds to the inter-quartile range; any slopes outside this range are considered outliers and represented as dot.

To determine if the variability in the slope was associated with any of the experimental factors: eccentricity, external noise level, or phase angle, a second ANOVA was conducted. The ANOVA model contained main effects for each of the three factors listed above: external noise (NSD), phase (Theta), and eccentricity (Ecc). Interaction terms were also included for external noise and phase, and external noise and eccentricity. Since differences in the slope appeared to be most closely related to the external noise level, these interaction terms were included to test the possibility that changes in slope depended on a second factor. An additional variance term was included to account for variability introduced by each observer so that this additional within subject variably was not interpreted as between subject variability. The outcome of the ANOVA is presented in Table (3.3) below. As expected, external noise was the only factor that could not be

ruled out as an account for the changes in slope of the psychometric functions. The lack of interaction between the external noise level and the phase relation suggested that any changes in the observer's strategy that were reflected in the slope of the psychometric function across high and low external noise levels did not depend on whether the stimuli were in sine or cosine phase.

	DF	Sum Sq	Mean Sq	F	Pr(>F)
Theta	1	0.16	0.16	0.92	0.34
NSD	4	3.051	0.76	4.44	0.0036
Ecc	4	0.224	0.056	0.326	0.859
NSD:Theta	4	0.292	0.073	0.424	0.790
NSD:Ecc	16	1.733	0.108	0.631	0.844
Residuals	53	9.103	0.172		

Table 3.2: ANOVA of effects on slope. The effects of the external noise (nsd), eccentricity (ecc), and phase (theta) on the slope of the psychometric functions are shown in the ANOVA table. To account for additional variability introduced by the individual observers, a random effect terms were added for the observers. Testing was performed at 5 levels of external noise (NSD), 5 levels eccentricity (not all observers were tested at all five levels), and two levels of phase (Theta).

3.3.4 Summary

The noise masking experiment reported in this section explored the influence of external noise on the observer's ability to performance discriminations in the sine and cosine conditions at both low and high eccentricities. Unlike previous results, the observer's threshold did not scale with level of external noise but rather tended to fluctuate considerably at low external noise levels before leveling off somewhat at high external noise. These inconsistencies in the shape

of the noise masking function meant that the slope and x-intercept parameters associated with this function were difficult to interpret. Consequently, there was no clear evidence to suggest that either an increase in the level of internal noise or a decrease in the observers sampling efficiency was associated with the decline in sine performance at high eccentricity based on the noise masking functions.

An ANOVA was also used to determine if the unusual shape of the noise masking function was related to the other experimental factors, eccentricity and phase. As expected, the threshold ANOVA indicated that there was an interaction between phase and eccentricity and a main effect of the external noise level. Despite some differences in the shape of the noise masking functions at high and low eccentricities, the ANOVA showed that main effect of external noise did not depend on either the eccentricity or phase, suggesting that the unusual shape of the noise masking function was consistent across the other two experimental factors. A second ANOVA was also performed to indicate if any of the three experimental factors influenced the slope of the psychometric function. Of these factors, only the external noise level had a main effect on the psychometric slope. The absence of any phase related effects in this ANOVA indicated that uncertainty might not have played much of a role in the distinguishing between performance in the sine and cosine condition at high eccentricity.

Overall, the results provided in this section revealed a clear influence of the external noise level on the observers response irrespective of the other experimental factors. The influences related to the phase, however, remained more difficult to disambiguate. Although there was some evidence that the usual shape of the

noise masking function was unlikely to be due to a combination of internal noise sources, the effect of phase and will be investigated in more detail in the next experiments.

3.4 Experiment 3: Response Consistency

The purpose of the third experiment was to examine if the disparity in performance between the sine and cosine conditions could be accounted for by differences in the internal noise level. To determine if the total amount of internal noise differed as the stimulus position was shifted from low to high eccentricity, an estimate of the internal noise level was provided using a response consistency method in which the observer performed two passes through an identical sequence of stimuli (Burgess and Colborne, 1988). Response consistency provides a direct measure of internal noise by measuring the observer's performance twice using the same sequence of external noise samples. Since the external noise is fixed across the two passes, any differences in the observer's response between the first and second pass are assumed to be the result of internal noise. Typically this method is used in combination with the noise masking function to separate out whether a change in the slope of the noise masking function corresponds to an additional contrast dependent source of internal noise or to a change in the observer's sampling efficiency. However, since the parameters of the noise masking function in the previous experiment were difficult to interpret due to inconsistencies in the observers' thresholds across external noise levels, response consistency provided an alternate method for estimating observers' internal noise that required measurement at only a single level of externally added noise.

3.4.1 Methods & Observers

Three trained observers (s04, s14, s21) participated in Experiment 2. As in Experiment 1, observers viewed the stimuli centrally and at one or more higher eccentricities. Each of the observers completed the task at the highest external noise level (nsd = $3.48e^{-6}$). A lower external noise level (nsd = $6.26e^{-7}$) was also used for one of the observers to determine if the level of internal noise varied from low to high external noise levels. The task in this experiment was modified from the first experiment so that, instead of a single pass through the stimulus sequence, observers performed two passes through the same sequence of 250 stimuli; i.e., an exact copy of the stimuli from each trial in the first pass was repeated in the second pass. Since the signal contrast in the second pass was determined by the staircase from the first pass, a staircase procedure was no longer necessary in the second pass. One of the observers, s04, also performed the task in a low noise (nsd = $6.26e^{-7}$) condition. This allowed for a comparison to be made between the internal-to-external noise ratios (I/E) at high and low external noise levels to determine if the internal noise level was dependent on the external noise level.

3.4.2 Results

The results from the response consistency experiments for the three observers are plotted in Figure (3.10). Overall, there did not appear to be any remarkable changes in the I/E ratio as the stimulus presentations were shifted into the parafovea. While there did appear to be some small individual differences in the internal noise levels between the sine and cosine conditions, these differences did

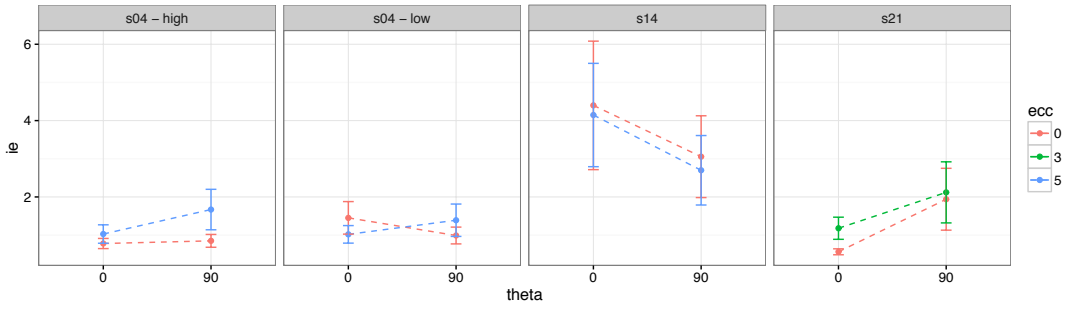

Figure 3.10: Response consistency. Estimates of the observers internal-to-external noise ratio (I/E) are plotted against the phase angle-0 corresponds to the cosine condition and 90 to the sine condition. The points are colored according to the eccentricity in degrees of visual angle. Errorbars extend to one standard deviation above and below the estimated ratio. These errorbars were calculated based on 1000 bootstrapped simulations of the estimated I/E ratio.

not reflect the large disparity in thresholds that separated the sine and cosine conditions when the stimuli appeared in the parafovea. For the observer that also participated in the low external noise condition, there did not appear to be a consistent difference between the I/E ratios at high and low noise. This suggests that, for this particular observer, the level of internal noise was not growing along with external noise. Therefore, based on the minor differences in the I/E ratios found in this experiment, only small changes in the observer's threshold are to be expected as the stimulus presentation was shifted from low to high eccentricity.

3.5 Experiment 4: Response Classification

In Experiment 4, the possibility was considered that the rapid decline in the observer's ability to make discriminations based on differences in relative spatial position under parafoveal viewing conditions was due to a shift in the observer's underlying template. Differences in the observer's template reveal changes in the observer's strategy for performing the task, and may be the result of perceptual

learning Gold et al. (2004). One change in the observer's strategy that has been found in previous experiments is that, due to the observers reliance on less sensitive regions of the visual field, observers relied on lower spatial frequencies to discriminate between pairs of stimuli (Levi and Klein, 2002; Thibos et al., 1996). In a similar classification image experiment involving grating patterns, Levi and Klein (2002) found that observers tended to overweight higher frequencies in the fovea and lower frequencies in the parafovea. The classification image provides an estimate of how the observer weighted each of the 128 'pixels' that made up the stimulus. In this final experiment, a classification image was computed for each stimulus pair in the fovea and periphery, resulting in a total of 4 classification images for each observer.

3.5.1 Observers

Three observers participated in this experiment: s04, s14, and s21. All of the observers were familiar with the task and stimuli prior to participating. Due to the extended nature of the experiment, observers were scheduled to participate over a 1 to 2 month period to obtain the required number of experimental trials.

3.5.2 Methods

The task and stimuli used in the classification image experiment was the same task that had been used in previous experiments (see section 2.5). Even though a threshold was not estimated in this experiment, the contrast level of the signal was still varied according to the same staircase procedure used in previous experiments to ensure that the classification images obtained were representative of the observer's template used throughout the experiments. The level of external noise

was fixed at the highest level (nsd = $6.26e^{-6}$). Classification images were estimated in both the sine and cosine conditions at high and low eccentricities. The high eccentricity condition for each observer corresponded to the same eccentricity used in previous experiments, which was determined during pilot experiments to be a point where the observer's performance noticeably declined. Since the signal varied along only the horizontal axis of the stimulus, noise was added to each of the 128 vertical lines that made up the stimulus. On each trial a different sample of noise was added to the signal in both presentation intervals. To provide a reliable estimate of the weights assigned to each of the 128 stimulus elements, an average of 5000 trials were conducted for each classification image. The trials were divided up into blocks of 1000 trials, for a total of about 20 blocks for each observer.

3.5.3 Results

The classification images that resulted by combining each of the 8 possible stimulus–response pairs according to their response type (see Figure 2.8) are plotted in Figure (3.11) below. The gray line shows the classification image surrounded by a dark gray region that extends to an estimate of plus and minus one standard deviation. The original signal is shown by the orange line. A closer match between the classification image estimate and the original signal indicates that the observer sampled more efficiently from the signal. Portions of the stimulus that were weighted more heavily by the observer correspond to larger amplitude portions (in both the positive and negative direction) of the classification image. These high amplitude portions reveal trends in the observer's strategy that are typically not discoverable using other methods. For example, in

some cases, particularly the sine condition, the edges of the stimulus were used for discrimination, whereas in the cosine condition the center of the stimulus was the preferred stimulus region.

The amplitude spectrum of each classification image is plotted in the panel below each figure. This spectrum indicates the amplitudes of sinusoids of different periodicities that appear within the classification image. For this particular task, the discriminative information was limited to the 2nd harmonic, which had a frequency of 4 cycles/image. In most of the conditions where the stimulus was presented in the fovea (columns 1 & 2) there was some evidence that the observer was making use of stimulus information in some or all of the peaks and troughs of the waveform. This evidence was available both by visual inspection and from the peak at 4 cycles/image in the amplitude spectrum. While the observation that observers tended to use all of the peaks and troughs of the second harmonic appears to hold for the first two observers when the stimulus was presented in the fovea, the observer in row three appeared to have some difficulty in the cosine condition. The classification image corresponding to this condition, in the bottom left, shows that the observer relied more on the edges of the stimulus than the central stimulus region.

As stimulus presentations were shifted beyond the centermost region of the visual field, the classification images appear noisier—reflecting increased spatial uncertainty associated with the parafoveal region of the visual field. The classification images and corresponding amplitude spectra from the 3rd and 4th columns of Figure (3.11) show a shift towards lower frequency components; the

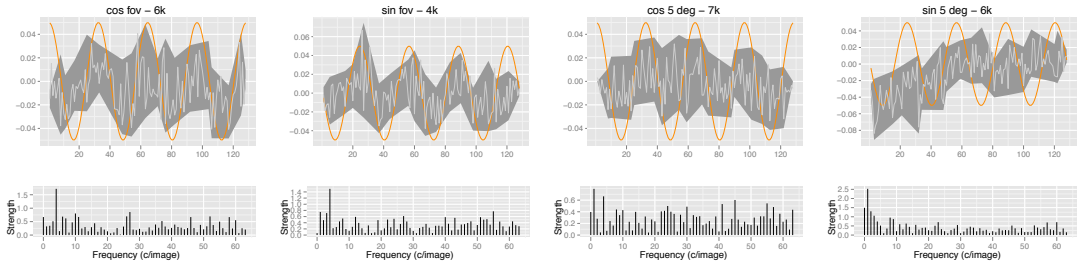

(a)

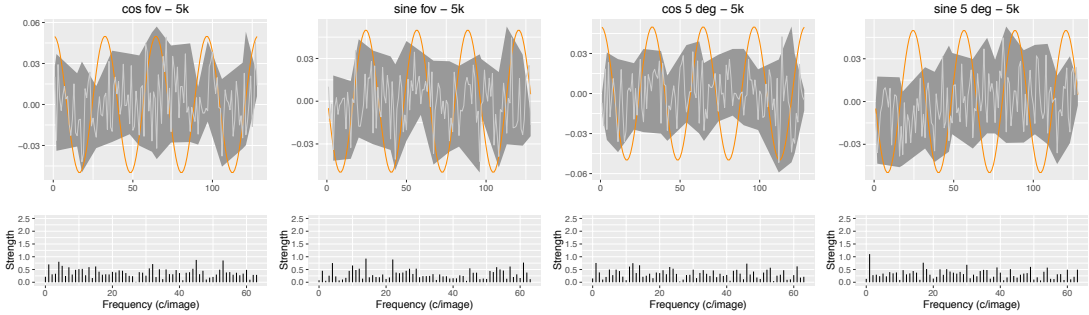

(b)

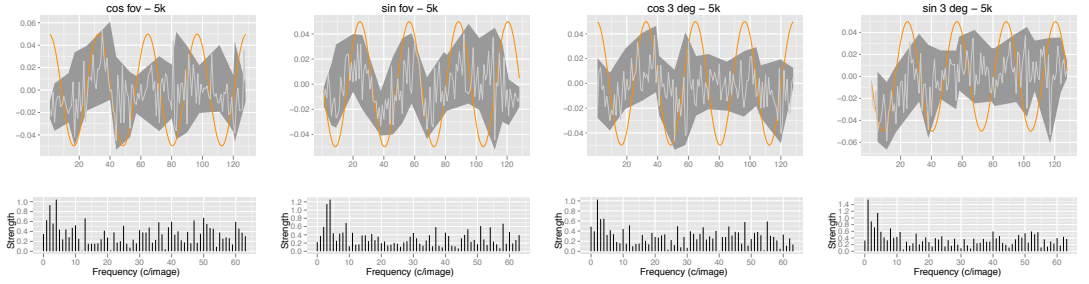

(c)

Figure 3.11: Classification images. The figure is separated into three rows or panels—one for each observer (s04, s14, s21, in that order). The phase relation (sine or cosine) along with the eccentricity and number of trials are indicated in the figure title. The actual classification image estimate shown by the light gray line, which falls a darker gray shaded region that represents an estimate of +/- one standard deviation of each point within the classification image. The corresponding one-sided amplitude spectrum is shown below each classification image.

first harmonic, in particular, tended to be more heavily weighted across the three observers. One potential strategy that relies on the 1st harmonic is to perform a light-dark comparison between the left and right halves of the stimulus. At least one observer reported being unable to perform the parafoveal task in the sine condition without making use of the left edge of the stimulus to perform a light-dark discrimination. Evidence for use of this strategy appears in the sine condition classification images for all three observers. Unlike the sine condition, the central portion of the stimulus tended to be weighted more than the edges in the cosine condition. This preference was consistent with a strategy in which a light-dark discrimination was performed using the central portion of the stimulus.

To determine if the templates estimated from these three observers differed from a random template, Hotellings T^2 test, which is a multivariate generalization of the more commonly used Student's t-test, was used. This test provides some indication of whether or not the classification image revealed that the observer made use of a consistent strategy to perform the task. Visually, regions of the stimulus that were strongly weighted by the observer indicate that the observer made consistent use of those regions. Statistically, strongly weights are less likely to occur by chance provided that the weighs were sampled from a normal distribution. Abbey and Eckstein (2002) have used this method to compare classification image estimates from similar psychophysical tasks using large samples of noise.

Based on the p-values from Table (3.3), a number of the classification image estimates were not distinguishable from noise alone. For example, observer

	s04	p-value
$\cos_0$	$T^2_{1,127} = 9.59$	0.0024
sine_0	$T^2_{1,127} = .094$	0.759
$\cos_5$	$T^2_{1,127} = 6.05$	0.0153
sine_5	$T^2_{1,127} = 29.27$	$3.01e^{-}7$

	s14	p-value
$\cos_0$	$T^2_{1,127} = 1.02$	0.31
sine_0	$T^2_{1,127} = .173$	0.67
$\cos_5$	$T^2_{1,127} = .60$	0.4395
sine_5	$T^2_{1,127} = .47$	0.49

	s21	p-value
$\cos_0$	$T^2_{1,127} = 2.96$	0.088
sine_0	$T^2_{1,127} = 1.27$	0.26
$\cos_5$	$T^2_{1,127} = 7.9$	0.0057
sine_5	$T^2_{1,127} = 2.05$	0.157

	s04	p-value
$\cos_0$-$\cos_5$	$T^2_{1,127} = .1.27$	0.26
sine_0-sine_5	$T^2_{1,127} = .15.9$	0.0001

	s21	p-value
$\cos_0$-$\cos_5$	$T^2_{1,127} = .41$	0.5254
sine_0-sine_5	$T^2_{1,127} = .136$	0.713

Table 3.3: Hotellings T^2 test. T^2 tests were conducted to determine if the estimated weights assigned each of the stimulus pixels differed from chance. The row labels in the first column of each table indicate the condition and the subscript indicates the eccentricity. The T^2 value for each test is shown in the second column along with the degrees of freedom as subscripts. The last column indicates the p-value, or the likelihood of obtaining a result at least or more extreme, associated with each test.

14 had low T^2 values across all 4 conditions. The template estimates from observer 21 were more distinguishable from chance in the cosine condition than the sine condition suggesting that this observer used a more reliable strategy in the cosine condition than in the sine condition. Observer 4 also used a distinct strategy in the both cosine conditions and in the high eccentricity sine condition. The strong weights estimated from the high eccentricity sine condition were most likely due to a reliance on the edge portion of stimulus. A second set of T^2 tests was performed based on the difference between the template estimated in the fovea and the template estimated in the parafovea for both the sine and cosine condition. This test was conducted to determine if there was evidence that the observer may have changed strategies in response to the change of stimulus position. These tests were conducted only for observers 21 and 4 since there was no evidence that observer 14 used a reliable strategy in either condition. The only significant effect in this set of interaction tests was that observer 4 showed a disparity in the sine condition. This test result is not surprising given the previous interpretation of observer 4's high-eccentricity sine strategy.

Overall, these classification images show that there was a clear distinction between the consistency of observer's strategies in the fovea and parafovea. With the exception of a preference for the edge of the stimulus in the sine condition at high eccentricity, other portions of the template estimate were largely indistinguishable from noise in the higher eccentricity condition, suggesting that there was considerable spatial uncertainty in both the sine and cosine conditions.

In terms of the explaining the difference between the sine and cosine con-

dition, which was the motivation behind these experiments, one possibility was that, consistent with the findings of Huang et al. (2006), performance in the high eccentricity condition could be described by a single channel model. Based on the template estimates in the sine condition, there was clear evidence that observers were performing the task based a very limited portion of the signal information, i.e., about half a cycle of the overall pattern. In this condition, by using the edge of the stimulus, observers were also making use of some information that was not necessarily part of the signal. This edge-based strategy did rely on the overall signal pattern, as predicted by a two-channel model, but rather a local contrast difference between the edge and the background. Hence, this strategy is more consistent with a single-channel model that is sensitive to differences at the peaks and troughs of the waveform (i.e., local contrast differences) than a two-channel model in which contrast differences are integrated across the entire stimulus. This model could also account for performance in the cosine condition since the discriminative information in the cosine condition fell within this channel. Template estimates in the cosine condition also appeared to resemble the signal pattern more closely than in the sine condition.

3.5.4 Spatial Aliasing

Another possibility to account for the rapid decline in performance in the sine relative to the cosine condition was that the task in the cosine condition was more akin to a detection task in which the observer simply needed to detect the presence or absence of a peak in the center of the grating pattern; whereas, the task in the sine condition was more like a discrimination task that required the observer to locate whether bright and dark bars had been shifted to the right or

left a fixed reference point on the screen. Given that greater spatial acuity was required to perform a discrimination task, spatial aliasing (i.e., undersampling of the retinal image) may have disproportionately affected performance in the sine relatively to the cosine condition. According to Thibos et al. (1987), the frequency resolution above which the signal is under sampled is considerably different for these two different types of tasks. At 5 degrees of eccentricity in the nasal field Thibos et al. (1987) found that the spatial frequency limit for detection was roughly 3 times greater than the limit for resolution (i.e., roughly 45 vs. 15 cycles/deg), and by 20 degrees of eccentricity this difference had approximately doubled to a 6-fold increase. While the actual resolution limit reported by these authors was comfortably above the spatial resolution of the stimuli used in these tasks, which was about 1 cycle/deg, the signals used in these tasks were also corrupted by external noise. In addition to obscuring the identity of the signal, the spatial resolution of the external noise (16 cycles/deg) also fell above the 15 cycles/deg resolution limit reported by Thibos et al. (1987) for a discrimination task at 5 degrees of eccentriticy, introducing the possibility that portions of the noise may have been aliased. Hence, there is reason to believe that the overall effects of noise and aliasing may have substantially reduced the observer's ability to resolve the underlying signal pattern in both conditions. Due to the observer's strong reliance on positional cues in the sine condition, this limitation may have resulted in a disproportionate reduction in performance in the sine condition.

3.5.5 Limitations

One of the main difficulties in determining how the difference between sine and cosine performance was expressed in terms of the observer's signal to noise

ratio was the amount of spatial uncertainty associated with the high eccentricity condition. Based on the classification image results from this condition, observers appeared to be unable to consistently make use of differences in the individual pixel intensities to perform the task. As indicated by the spectral analysis of these images, observers instead tended to focus on differences incorporating broader regions of the signal. For example, observers may have performed the task by comparing whether the first pattern appeared to be lighter or darker than the second pattern. According to this interpretation, observers were no longer performing a phase discrimination task; instead they are taking advantage of local cues in the luminance profile of the signal to perform the task. Since the classification image method takes advantage of correlations at the individual pixel level to reveal trends in the observer's strategy, it was not entirely clear from this analysis how the observers underlying template was changing between the sine and cosine condition other than a preference for the edge portion of the signal in sine condition.

3.6 Summary

Broadly speaking, the results of the four experiments presented in this chapter provide evidence for several claims about the perceptual changes that occur as the presentation of a pattern is shifted outward from the fovea. In the first experiment, evidence was provided that sine-related patterns were more difficult to discriminate from their mirror-image counterparts than cosine patterns from their asymmetric counterparts. This finding could be easily replicated on trained psychophysical observers, and to a lesser extent, on naive observers. In

Experiment 2, raising the external noise level was shown to have an inconsistent (i.e., non-linear) effect on thresholds. The unusual shape of the noise masking function raised some doubts as to whether the parameters typically used to describe the noise masking function (i.e., slope and negative x-intercept) could be meaningfully interpreted. A third experiment was conducted to provide a separate estimate of the internal noise levels at high and low eccentricity. Results from this experiment, which found minimal differences in the internal to external noise ratio across eccentricities, combined with the irregular shape of the noise masking functions suggested that the deficiency in sine-related discriminations was unlikely to be due to an increase in the amount of internal noise limiting performance. However, some clear differences between the pattern of the observer's responses in the sine and cosine condition finally emerged in the response classification experiment. The classification images estimated in this experiment, while noisy (particularly in the high eccentricity condition), did show that observers appeared to rely on a smaller portion of the signal in the sine than the cosine condition. One possible account for observers' reliance on the edge portion of the signal in the sine condition at high eccentricities was that, unlike the rest of signal, this portion allowed observers to perform the task based on whether the edge was light or dark instead of having to perform a more complicated task of determining whether the bars were ordered from light to dark or dark to light—i.e., the edge may have allowed observers to perform a simple contrast discrimination rather than a relative phase discrimination.

Overall, the disparity observed in these experiments between the physical characteristics of the stimulus and the perceptual ability of the observer suggests

that there are fundamental differences in the way that observers make use of visual information in their parafovea, and that these differences cannot be easily described in terms of internal noise or the sampling efficiency. Nevertheless, these concepts provide a good starting point for understanding how the observer's sensitivity to contrast and spatial position differ between central and parafoveal vision. In particular, observers tend to locate portions of the stimulus that allow them to perform simpler contrast discriminations as opposed to more complicated global discriminations that rely on more precise spatial position in the fovea. Further experiments are necessary to determine if there are more effective mappings between the observer's visual sensitivity in regions beyond the fovea to the stimulus information.

3.7 Future Directions

The results of this thesis suggest that further experiments are necessary to arrive at a better understanding of how phase differences influence our perception of a pattern in visual regions beyond the fovea. While the methods employed in this thesis are well suited for identifying changes in the factors limiting the observers performance in the fovea, experimental results obtained using these techniques are more difficult to interpret when applied to visual regions outside of the fovea with high spatial uncertainty.

Two methodological changes that would be made if these experiments were repeated. The first change would be to select different levels of external noise. In the foveal condition, the task appeared to be too easy for observers in the

low noise levels, and in the high eccentricity condition the task was likely too difficult for observers. To strike a balance between these two conditions, different ranges of external noise could be used for the two conditions with some overlap. Fewer levels of external noise also could have been used. This change might have made the ANOVA more revealing by introducing fewer degrees of freedom for the interaction terms. The second change would have been to more effectively remove the edge effects from the stimulus. Using a narrower Gaussian envelope would have helped diminish the signal at the edge more effectively.

Future experiments might be more effective by moving away from models that assume a high level of spatial accuracy so that methods such Fourier analysis can be used to examine the observer's frequency response. Instead, less complicated models might be developed that involve simpler comparisons such as light-dark or left-right discriminations to build up a more complicated set of visual features. Based on the findings of these experiments, left-right discriminations would be more difficult for the observer than light-dark discriminations. A simple test experiment would be to measure the minimum contrast necessary for the observer to perform these two types of discriminations.

Another step in this process would be to rethink the way noise can be used to provide a more meaningful correlation with the observer's strategy at high eccentricity. One obvious possibility would simply be to enlarge stimuli and noise features to make them more visible and therefore more likely to influence the observer's response. Other possibilities might be to reorder the features or change their spatial position to examine if there are certain arrangements of stimulus

elements that are distinguishable at high eccentricities. These experiments could be done using simple block-like stimuli that would be easier to for the observer to distinguish in the parafovea. Building on the findings from this thesis, future experiments would be designed to operate on the similar spatial scale as visual regions such as the parafovea to better understand the perceptual constraints at higher eccentricities.

4 | Bibliography

Abbey, C. K. and Eckstein, M. P. (2002). Classification image analysis: Estimation and statistical inference for two-alternative forced-choice experiments. *Journal of vision*, 2(1):5–5.

Abbey, C. K. and Eckstein, M. P. (2009). Frequency tuning of perceptual templates changes with noise magnitude. *JOSA A*, 26(11):B72–B83.

Ahumada, A. J. (2002). Classification image weights and internal noise level estimation. *Journal of Vision*, 2(1).

Badcock, D. R. (1984). How do we discriminate relative spatial phase? *Vision research*, 24(12):1847–1857.

Beard, B. L. and Ahumada Jr, A. J. (1998). Technique to extract relevant image features for visual tasks. In *Photonics West'98 Electronic Imaging*, pages 79–85. International Society for Optics and Photonics.

Bennett, P. J. and Banks, M. S. (1987). Sensitivity loss in odd-symmetric mechanisms and phase anomalies in peripheral vision. *Nature*, 326(6116):873–876.

Bennett, P. J. and Banks, M. S. (1991). The effects of contrast, spatial scale, and orientation on foveal and peripheral phase discrimination. *Vision research*, 31(10):1759–1786.

Blakemore, C. and Campbell, F. W. (1969). On the existence of neurones in the human visual system selectively sensitive to the orientation and size of retinal images. *The Journal of Physiology*, 203(1):237–260.

Bracewell, R. N. (1989). The fourier transform. *Scientific American*, 260(6):86–95.

Brainard, D. H., Pelli, D. G., and Robson, T. (2002). *Display Characterization*. John Wiley & Sons, Inc.

Burgess, A. E. and Colborne, B. (1988). Visual signal detection. iv. observer inconsistency. *J. Opt. Soc. Am. A*, 5(4):617–627.

Burr, D. C. (1980). Sensitivity to spatial phase. *Vision research*, 20(5):391–396.

Campbell, F. W. and Robson, J. G. (1968). Application of fourier analysis to the visibility of gratings. *The Journal of Physiology*, 197(3):551–566.

Cornsweet, T. N. (1962). The staircase-method in psychophysics. *The American journal of psychology*, 75(3):485–491.

DeValois, K. K. (1977). Spatial frequency adaptation can enhance contrast sensitivity. *Vision Research*, 17(9):1057 – 1065.

Efron, B. and Tibshirani, R. J. (1994). *An introduction to the bootstrap*. CRC press.

Field, D. J. and Nachmias, J. (1984). Phase reversal discrimination. *Vision Research*, 24(4):333–340.

Gold, J. M., Sekuler, A. B., and Bennett, P. J. (2004). Characterizing perceptual learning with external noise. *Cognitive Science*, 28(2):167–207.

Graham, N. and Nachmias, J. (1971). Detection of grating patterns containing two spatial frequencies: A comparison of single-channel and multiple-channels models. *Vision Research*, 11(3):251 – IN4.

Graham, N., Robson, J., and Nachmias, J. (1978). Grating summation in fovea and periphery. *Vision Research*, 18(7):815 – 825.

Green, D. and Swets, J. (1966). *Signal Detection Theory and Psychophysics*. New York: Wiley.

Green, D. M. (1964). Consistency of auditory detection judgments. *Psychological review*, 71(5):392.

Harvey, L. O., Rentschler, I., and Weiss, C. (1985). Sensitivity to phase distortions in central and peripheral vision. *Attention, Perception, & Psychophysics*, 38(5):392–396.

Huang, P.-C., Kingdom, F., and Hess, R. (2006). Only two phase mechanisms,±cosine, in human vision. *Vision research*, 46(13):2069–2081.

Hubel, D. H. and Wiesel, T. N. (1974). Uniformity of monkey striate cortex: a parallel relationship between field size, scatter, and magnification factor. *Journal of Comparative Neurology*, 158(3):295–305.

Klein, S. A. (1992). Channels in the visual nervous system: Neurophysiology, psychophysics and model. *Channels: Bandwidth, channel independence, detection vs discrimination, B. Blum, Ed*, pages 11–27.

Knoblauch, K. and Maloney, L. T. (2012). *Modeling psychophysical data in R*, volume 32. Springer Science & Business Media.

Koenderink, J. and Doorn, A. v. (1978). Visual detection of spatial contrast; influence of location in the visual field, target extent and illuminance level. *Biological Cybernetics*, 30(3):157–167.

Legge, G. E., Kersten, D., and Burgess, A. E. (1987). Contrast discrimination in noise. *JOSA A*, 4(2):391–404.

Levi, D. M. and Klein, S. A. (2002). Classification images for detection and position discrimination in the fovea and parafovea. *Journal of Vision*, 2(1):4–4.

Levitt, H. (1971). Transformed up-down methods in psychoacoustics. *The Journal of the Acoustical society of America*, 49(2B):467–477.

Murray, R. F. (2011). Classification images: A review. *Journal of Vision*, 11(5).

Nachmias, J. and Weber, A. (1975). Discrimination of simple and complex gratings. *Vision research*, 15(2):217–223.

Oppenheim, A. V. and Lim, J. S. (1981). The importance of phase in signals. *Proceedings of the IEEE*, 69(5):529–541.

Pantle, A. and Sekuler, R. (1968). Size-detecting mechanisms in human vision. *Science*, 162(3858):pp. 1146–1148.

Peli, E. (1990). Contrast in complex images. *JOSA A*, 7(10):2032–2040.

Pelli, D. and Blakemore, C. (1990). The quantum efficiency of vision. *Vision: Coding and efficiency*, pages 3–24.

Pelli, D. G. (1981). *Effects of visual noise*. PhD thesis, University of Cambridge.

Pelli, D. G. and Farell, B. (1999). Why use noise? *J. Opt. Soc. Am. A*, 16(3):647–653.

Purves, D., Augustine, G., Fitzpatrick, D., Katz, L., LaMantia, A., McNamara, J., and Williams, S. (2001). Neuroscience. second. *Sunderland: Sinauer*.

Rentschler, I. and Treutwein, B. (1985). Loss of spatial phase relationships in extrafoveal vision. *Nature*.

Rovamo, J. and Virsu, V. (1979). An estimation and application of the human cortical magnification factor. *Experimental brain research*, 37(3):495–510.

Spiegel, M. F. and Green, D. M. (1981). Two procedures for estimating internal noise. *The Journal of the Acoustical Society of America*, 70(1):69–73.

Stromeyer, C. and Klein, S. (1974). Spatial frequency channels in human vision as asymmetric (edge) mechanisms. *Vision Research*, 14(12):1409 – 1420.

Swanson, W. H. and Fish, G. E. (1995). Color matches in diseased eyes with good acuity: detection of deficits in cone optical density and in chromatic discrimination. *JOSA A*, 12(10):2230–2236.

Tanner Jr, W. P. and Birdsall, T. G. (1958). Definitions of d and η as psychophysical measures. *The Journal of the Acoustical society of America*, 30(10):922–928.

Thibos, L., Cheney, F., and Walsh, D. (1987). Retinal limits to the detection and resolution of gratings. *JOSA A*, 4(8):1524–1529.

Thibos, L. N. and Bradley, A. (1991). The limits of performance in central and peripheral vision. *SID91 Digest of Technical Papers*, 22:301–303.

Thibos, L. N., Still, D. L., and Bradley, A. (1996). Characterization of spatial aliasing and contrast sensitivity in peripheral vision. *Vision research*, 36(2):249–258.

Tjan, B. S., Braje, W. L., Legge, G. E., and Kersten, D. (1995). Human efficiency for recognizing 3-d objects in luminance noise. *Vision Research*, 35(21):3053 – 3069.

Tolhurst, D. and Barfield, L. (1978). Interactions between spatial frequency channels. *Vision Research*, 18(8):951 – 958.

SHAWN BARR

sbarr2@gmail.com

EDUCATION

PhD, Psychological & Brain Sciences 2017
Statistics Minor
Indiana University – Bloomington, IN

BA, Psychology 2007
Biochemistry Minor
Clark University – Worcester, MA

Non-degree, Computer Science, University of New Mexico – Los Alamos, NM 2009
Complex Systems Summer School, Santa Fe Institute, Santa Fe, NM 2008

WORK EXPERIENCE

Biomedical Data Analyst May 2016–Present
SleepIQ Labs – San Jose, CA

Post-baccalaureate Researcher 2008–2010
Petavision Project
New Mexico Consortium/Los Alamos National Laboratory, Los Alamos, NM

Developer/Intern 2007–2008
Redfish Group – Santa Fe, NM

PUBLICATIONS

Bratch, A., Barr, S., Bromfield, W. D., Srinath, A., Zhang, J., & Gold, J. M. (2016). The impact of configural superiority on the processing of spatial information. *Journal of Experimental Psychology: Human Perception and Performance*, 42(9), 1388.

Barr, S., & Gold, J. M. (2014). Redundant visual information enhances group decisions. *Journal of Experimental Psychology: Human Perception and Performance*, 40(6), 2124.

Gold, J. M., Barker, J. D., Barr, S., Bittner, J. L., Bratch, A., Bromfield, W. D., ... & Srinath, A. (2014). The perception of a familiar face is no more than the sum of its parts. *Psychonomic Bulletin & Review*, 1-8.

Gold, J. M., Barker, J. D., Barr, S., Bittner, J. L., Bromfield, W. D., Chu, N., ... & Srinath, A. (2013). The efficiency of dynamic and static facial expression recognition. *Journal of Vision*, 13(5).

Gintautas, V., Ham, M. I., Kunsberg, B., Barr, S., Brumby, S. P., Rasmussen, C., ... & Kenyon, G. T. (2011). Model Cortical Association Fields Account for the Time Course and Dependence on Target Complexity of Human Contour Perception. *PLoS computational biology*, 7(10), e1002162.

Joyce, David, Kennison, John, Densmore, Owen, Guerin, Steven, Barr, Shawn, Charles, Eric and et al. (2006). My-way Or The Highway: a More Naturalistic Model of Altruism Tested in an Iterative Prisoners' Dilemma. *Journal of Artifical Societies and Social Simulation* 9(2).

TEACHING ASSISTANT EXPERIENCE

P211 – Research Methods Instructor
C105 – Pigskin, Probability, & Prediction
K300 – Statistics
P335 – Cognitive Psychology
P457 – Implementing Computer Controlled Experiments
P466 – Molecular & Cellular Neurobiology

PROGRAMMING EXPERIENCE

R, MATLAB, Python, Unix, Java, Scheme, MySQL, EMACS, LaTeX